
This is an electronic reprint of the original article.
This reprint may differ from the original in pagination and typographic detail.

Yu, Cunming; Sasic, Srdjan; Liu, Kai; Salameh, Samir; Ras, Robin H.A.; van Ommen, J. Ruud
Nature-Inspired self-cleaning surfaces

Published in:
Chemical Engineering Research and Design

DOI:
[10.1016/j.cherd.2019.11.038](https://doi.org/10.1016/j.cherd.2019.11.038)

Published: 01/03/2020

Document Version
Peer reviewed version

Published under the following license:
CC BY-NC-ND

Please cite the original version:
Yu, C., Sasic, S., Liu, K., Salameh, S., Ras, R. H. A., & van Ommen, J. R. (2020). Nature-Inspired self-cleaning surfaces: Mechanisms, modelling, and manufacturing. *Chemical Engineering Research and Design*, 155, 48-65. <https://doi.org/10.1016/j.cherd.2019.11.038>

This material is protected by copyright and other intellectual property rights, and duplication or sale of all or part of any of the repository collections is not permitted, except that material may be duplicated by you for your research use or educational purposes in electronic or print form. You must obtain permission for any other use. Electronic or print copies may not be offered, whether for sale or otherwise to anyone who is not an authorised user.

Nature-Inspired Self-Cleaning Surfaces: Mechanisms, Modelling, and Manufacturing

Cunming Yu^{a,*}, Srdjan Sasic^b, Kai Liu^c, Samir Salameh^{d,e}, Robin H.A. Ras^{e,f}, J. Ruud van Ommen^{d,*}

^a Key Laboratory of Bio-inspired Smart Interfacial Science and Technology of Ministry of Education, School of Chemistry, Beihang University, Beijing 100191, China

^b Department of Mechanics and Maritime Sciences - Division of Fluid Dynamics, Chalmers University of Technology, Gothenburg, Sweden

^c Department of Applied Physics, Aalto University School of Science, 02150 Espoo, Finland

^d Department of Chemical Engineering, TU Delft Process Technology Institute, Delft University of Technology, Delft, the Netherlands

^e Saint-Gobain Research Germany, Glasstraße 1, D -52134 Herzogenrath, Germany

^f Department of Bioproducts and Biosystems, Aalto University School of Chemical Engineering, 02150 Espoo, Finland

* Corresponding authors: ycmbhs@iccas.ac.cn; J.R.vanOmmen@tudelft.nl

Abstract

Nature-inspired self-cleaning surfaces have attracted considerable attention from both fundamental research and practical applications. This review adopts a chemical-engineering point of view and focuses on mechanisms, modelling, and manufacturing (M3) of nature-inspired self-cleaning surfaces. We will introduce six nature-inspired self-cleaning mechanisms: The Lotus-effect, superhydrophobic-induced droplet jumping, superhydrophobic-induced unidirectional movement of water droplet, underwater-superoleophobic-based self-cleaning, slippery-based self-cleaning, and dry self-cleaning. These mechanisms of nature self-cleaning examples are popular and well-known as well as have been widely applied or exhibited potential applications in our daily life and industrial productions. The mathematical and numerical modelling of the identified self-cleaning mechanisms will be carefully introduced, which will contribute to the rational design and reproducible construction of these functional self-cleaning surfaces. Finally, we will discuss how these materials can be produced, with a focus on scalable manufacturing. We hope this review will strengthen the understanding on nature-inspired self-cleaning surfaces and stimulate interdisciplinary collaboration of material science, biology and engineering.

Keywords: Bio-inspired, repellent, fundamentals, simulations, scalable production

1. Introduction

After billions of years of evolution, natural organisms have evolved intriguing surface self-cleaning properties. As one of the most famous self-cleaning biomaterials, Lotus leaf (*Nelumbo Nucifera*) has been recognized as the symbol of purity in Asian regions and cultures for more than 2000 years. Lotus

roots grow in mud, while its leaves are never dirty because of their special surface wettability: they exhibit superhydrophobicity-induced self-cleaning (Barthlott and Ehler, 1977). Only since the introduction of the scanning electron microscope (SEM) in 1970s, the detailed structures at the plant surface and their role in the surface functionalities could be

investigated (Schill et al., 1973.; Barthlott and Capesius, 1976). In 1997, the Lotus-effect was first studied in detail using SEM; self-cleaning behaviour is determined by the micro-scale papillae and the epicuticular wax (Barthlott and Neinhuis, 1997). In 2002, Feng et al. reported that micro/nano hierarchical structures, *i.e.*, branch-like nanostructures on top of the micropapillae, are essential in building up the superhydrophobic effect (Feng et al., 2002).

Apart from the Lotus-effect, which can safely be regarded as the most famous example of a self-cleaning mechanism, there are five more self-cleaning mechanisms that are clearly nature-inspired. Firstly, the drop-jumping mechanism, which can find inspiration from mosquito eyes, cicada wings, water strider legs, and so on (Gao et al., 2007; Wisdom et al., 2013; Wang et al., 2015). Secondly, the superhydrophobic-induced unidirectional movement of droplets on butterfly wings and bird's feathers (Kennedy 1970; Liu et al. 2008). Thirdly, the underwater-superoleophobic-based self-cleaning mechanism that are inspired by underwater organisms, *e.g.*, carp scale, the inner side of Columnar Nacre, and the lower surface of lotus leaf (Liu et al., 2009; Guo et al., 2016; Cheng et al., 2011.). Fourth is the slippery-based self-cleaning mechanism (Wong et al., 2011; Xiao et al., 2013; Cao et al., 2015). In nature, this mechanism is used by pitcher plants, a type of carnivorous plants. The last one is the dry self-cleaning mechanism, which is inspired by the structure of Gecko feet (Hansen and Autumn, 2005).

There exist a broad range of devices and situations in which there is a need for a working surface that reduces or even prevents the adhesion of different contaminants, such as dirt, organic matter or liquids. Applications of such a technology are numerous: from camera lenses and car windshields to preventing icing on planes, to name a few (Bhushan and Jung, 2011). It is thus not surprising that we have witnessed a significant development of the self-cleaning technology in recent years.

Only around 2005, the number of publications on this topic strongly increased, due to the availability of nanotechnological manufacturing techniques that enabled mimicking the Lotus-effect on artificial surfaces. Apart from technology-push, there is also an important market-pull factor: self-cleaning surfaces can contribute in several ways to the energy transition. For example, the substantial increase in displays and photovoltaic (PV) solar panels makes it attractive to have better self-cleaning materials (Yao and He, 2014). Worldwide, the installed PV capacity currently shows an annual growth of around 30 % (Masson et al., 2018). The performance of these PV panels, besides their lifetime, is also partly determined by how clean their surface is. As application is especially attractive in regions with strong sunlight, which are often also dry and dusty, providing these surfaces with good self-cleaning functionality would boost their performance. Fouling of these devices involving the cooling and cleaning of hydrocarbon-rich gases is a problem in numerous industrial applications, and it is considered responsible for 1 - 2.5 % of the global anthropogenic emissions of CO₂ (Müller -Steinhagen et al., 2009). Overall, heat exchanger fouling has been estimated to cost industrialized nations approximately 0.25 % of GDP (Müller -Steinhagen et al., 2005). It is thus clear that it is of great interest to facilitate self-cleaning of heat exchangers instead of cleaning them manually, which is not only tedious but would also require frequent interruptions in the plant operations. Since 2005, a number of reviews have been written about self-cleaning fields (Parkin and Palgrave, 2005; Quéé 2008; Bhushan et al., 2011; Ganesh et al., 2011; Liu and Jiang, 2012). Mostly the focus was either on the materials aspects or on the mechanisms. Given the readership of the current journal, we would like to approach the topic more from a chemical-engineering point of view. This means that, unlike most other reviews, we will pay substantial attention to model the self-cleaning mechanisms, and to the possibilities of large-scale manufacturing of

such materials. In brief, we will focus on mechanisms, modelling, and manufacturing (M3). Self-cleaning materials that are not clearly nature-inspired, such as photocatalytic surfaces, will not be considered in this review. The notion of Lotus-inspired superhydrophobicity will receive the most attention, since it has been most widely studied and applied. In addition, we will also discuss superoleophobicity, slippery-based self-cleaning, and dry self-cleaning. We will first discuss for each of the mechanisms how they were discovered, and how they can be translated from nature to man-made materials. Subsequently, we will discuss mathematical modelling of the different self-cleaning mechanisms, as this will aid the understanding and the design of future materials with even better performance. Finally, we will discuss how these materials can be produced, with a focus on scalable manufacturing.

2. Mechanisms for nature-inspired

self-cleaning phenomena

2.1. Superhydrophobicity-induced self-cleaning mechanisms

2.1.1. Lotus effect

The Lotus leaf can be considered the most famous inspiration from nature for the design of self-cleaning surfaces. As mentioned in the introduction, it relies on superhydrophobicity to remove mud or dirt by water or rain (**Figure 1a**). The underlying mechanism of Lotus leaf's self-cleaning property was first explored by Barthlott and Neinhuis in 1997 (Barthlott and Neinhuis, 1997). It was found that micrometer-scale papillae and epicuticular wax play an important role in its superhydrophobicity, *i.e.*, high water contact angle ($\sim 160^\circ$) and low sliding angle ($\sim 2^\circ$), which was defined as "Lotus effect" (Neinhuis and Barthlott, 1997). As shown in **Figure 1b**, the micro-sized papillae with diameters ranging from $5\ \mu\text{m}$ to $9\ \mu\text{m}$ are randomly distributed on the lotus

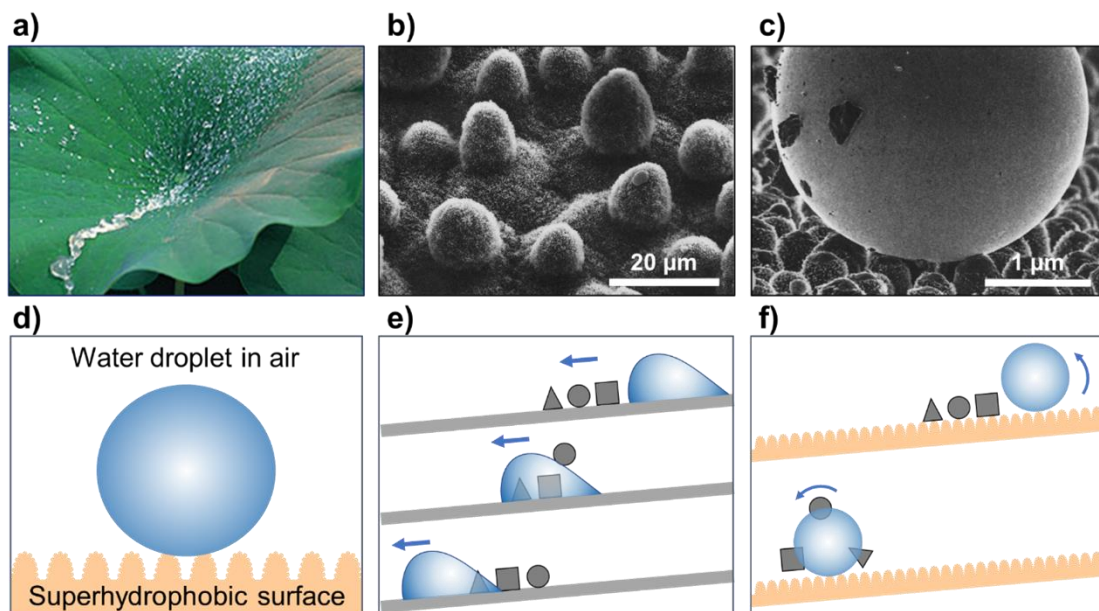


Figure 1. The Lotus effect is the most famous example of a superhydrophobicity-based self-cleaning mechanism. a) Water droplets are rolling across the lotus leaf surface and taking the dirt particles away, demonstrating the distinguished self-cleaning effect. b) SEM images of distributed cell papillae on the lotus leaf surface. c) Contaminating particles adhere to the surface of the droplet and are removed from the leaf when the droplet rolls off. d) Schematic illustration of Lotus state (a special case of Cassie's superhydrophobic state). e, f) Schematic illustration of water-droplet cleaning on smooth and structured surfaces, respectively. On the smooth surface, the particles are mainly only redistributed by water, while they adhere to the droplets' surfaces and are taken away from the rough surface. (Barthlott and Neinhuis, 1997) Copyright © 1997, Springer-Verlag Berlin Heidelberg.

leaf. However, the fundamental mechanism of its self-cleaning phenomenon was still not fully clarified. In 2002, Jiang et al. reported the nano-structures on every papilla, *i.e.*, fine branch-like nanostructures with a diameter of approximately 120 nm, which can greatly increase the roughness of lotus surface and effectively prevent the attachment of water droplets (Feng et al., 2002). When droplets rolled on the tips of epicuticular wax crystals on the top of papillose epidermal cells, contaminating particles will be attached on the droplets and carried away (**Figure 1c**). In general, there are two kinds of wetting states to define the superhydrophobic surface, *i.e.*, Wenzel's state and Cassie's state (Wenzel, 1935; Cassie and Baxter, 1944). In Wenzel's state, the water droplets pin to the surface in a wet-contact mode, and as a result, high contact angle (CA) hysteresis is observed. In contrast, in Cassie's state, the water droplets adopt a non-wet-contact mode on solid surfaces and can roll off easily owing to their low adhesive force. The "Lotus" effect is one representative example of superhydrophobic surfaces in Cassie's state (**Figure 1d**). Owing to micro/nano hierarchical structures and low-surface-tension energy, water droplets will have a very small contact area with superhydrophobic surfaces (2 % ~ 3 %). Similarly, the contact area of mud or dirt on a Lotus leaf is also very small, because mud and dirt are typically larger than the micro/nano structures of the Lotus leaf, which will be endowed with low adhesive force to a solid surface. However, the adhesive forces between mud or dirt particles with water droplet are relatively large resulting from their easy wetting property. Thus, mud or dirt particles on a superhydrophobic surface will be easily taken away by water droplets (**Figure 1f**). In contrast, on solid smooth surfaces, the contact area of mud or dirt particles is large, which will result in a huge adhesive force. Consequently, the adhesive force caused by water wetting is not large enough to take the particles away but will only regulate their positions (**Figure 1e**).

2.1.2. Droplet jumping phenomena (mosquito eyes, cicada wings, water strider legs)

Lotus-inspired superhydrophobic self-cleaning suffers from instability, because of the air sandwiched between the water and the micro/nano structures is replaced by water in the case of fog and dew (Cheng, 2005; Liu and Choi, 2013). Autonomous self-cleaning is achieved by a fascinating phenomenon of the self-propelled, coalescence-induced jumping motion of condensed water droplets that partially cover or fully enclose a contaminant particle to be removed and where no external fields (e.g. gravity) are needed. Nice examples from nature are the cleaning of surfaces such as mosquito eyes, lacewings, cicada wings, and water-strider legs (Helbig et al., 2011; Watson et al., 2011). There, small droplets are formed from the dew in places with no precipitation and are afterwards self-propelled from the surface after droplets touch each other. The chain of events is therefore straightforward and similar for both biological and synthetic surfaces: when water vapour condenses on superhydrophobic surfaces, the droplets will coalesce and the resulting droplet may jump from the surface as a result of the excess surface energy (Boreyko et al., 2009; Miljkovic et al., 2013; Kim et al., 2015). The jumping droplets are smaller than the capillary length (capillary length is about 2.7 mm for water) and are typically up to 100 μm large (Miljkovic et al., 2013) and, as indicated before, external forces (e.g. gravity) play no role in this type of self-cleaning. There are three mechanisms behind droplet jumping (Kim et al., 2015): 1) coalescence of two neighbouring droplets; 2) coalescence among more than two neighbouring droplets and 3) coalescence between one or more droplets on the surface and a returning droplet that has already departed.

As shown in **Figure 2a**, in 2007, Gao et al. reported the compound eyes of the mosquito *C. pipiens* can be capable of possessing ideal superhydrophobic property in fog environment, which is mainly attributed to

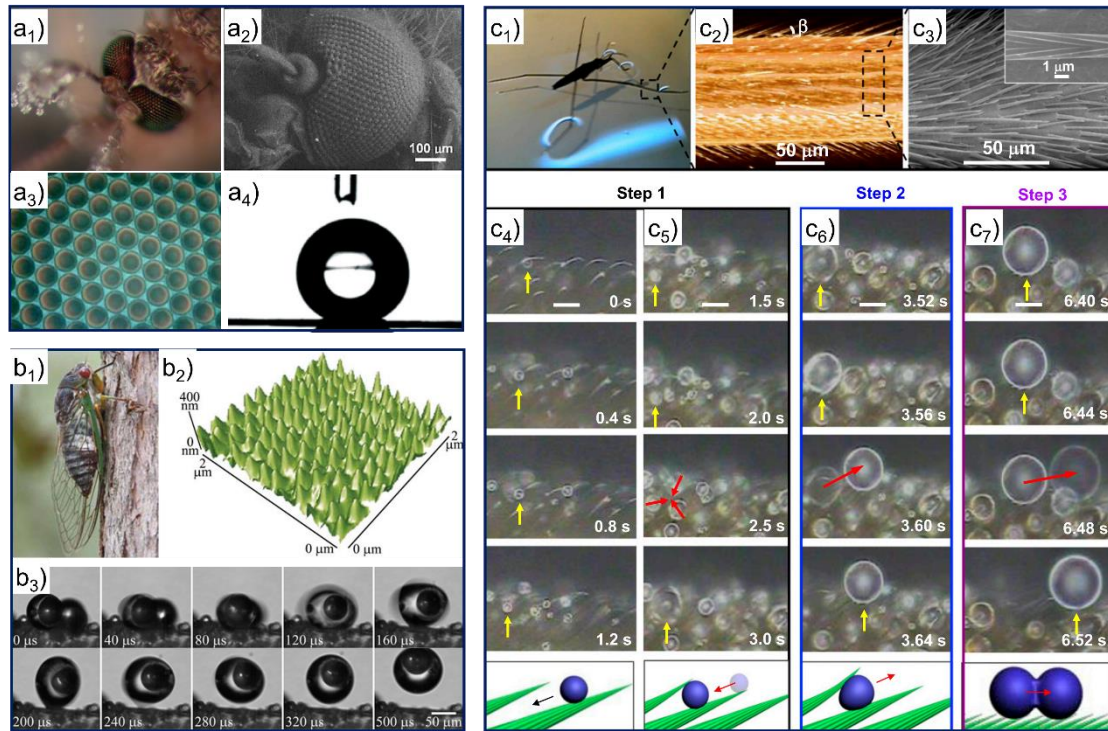


Figure 2. Natural examples of droplet jumping phenomena. a) The antifogging mosquito eyes and the related bioinspired surfaces (Gao et al. 2007). Copyright © 2007, Wiley-VCH. a₁. Optical image of antifogging mosquito eyes. a₂. SEM image of mosquito eyes. a₃. Optical image of artificial mosquito compound-eyes. a₄. Water droplet contact angle on artificial mosquito compound-eyes. b) Superhydrophobic cicada wing and droplet jumping process (Wisdom et al., 2013). Copyright © 2013, National Academy of Sciences. b₁. The cicada is usually oriented skyward when at rest. b₁. The wing is superhydrophobic because of the nanostructured surface shown by an atomic force microscope (AFM) image. b₃. Removal of a very hydrophilic glass particle of 50 μm by a jumping droplet. c) Self-motions of water droplets condensing on a leg of water strider (Wang et al., 2015). Copyright © 2013, National Academy of Sciences. c₁ ~ c₃. Optical image, Micro-XCT, and SEM images of a strider's leg. c₄ ~ c₇. Cascade of self-motions for water droplets condensing on a leg of water strider.

the hexagonally non-close-packed (NCP) nipples at the nanoscale preventing the microscale fog drops from condensing on the ommatidia surface (Gao et al., 2007). An example, i.e., superhydrophobic cicada wing, is shown in **Figure 2b**, where a 50 μm glass particle is removed from a superhydrophobic surface by a jumping droplet of a similar size. Different mechanisms of particle removal were identified in (Wisdom et al., 2013), primarily dependent on the degree of hydrophilicity of the particle: floating (for a very hydrophilic particle and shown in Figure 2b), lifting (the case of a less hydrophilic particle) and aggregating. The same study showed that the jumping-droplet removal mechanism is sufficient to achieve an autonomous self-cleaning function (i.e. no gravity or any other external effect were needed). In 2015, Wang et al. also reported that condensed water droplets of volume

ranging from femtoliter to microliter can be self-removed from the legs of water striders, which is mainly attributed to the elastic expulsion between flexible setae (Wang et al., 2015). Finally, it is worth noting that it has been demonstrated that the jumping droplet condensation also enhances heat transfer and promotes anti-icing (Kim et al., 2015).

2.1.3 Unidirectional droplet movement (e.g., butterfly wings, bird feathers)

Nature organisms with superhydrophobic surfaces also illustrate distinct unidirectional adhesive properties, i.e. the rolling and pinning states of a droplet may coexist on the same surface under different conditions. In 2007, Zheng et al. were first to report the unidirectional droplet movement on the superhydrophobic wings of the butterfly (*Morpho aega*), that is the droplet can easily roll off the wings along the radial outward (RO) direction of the central axis of the body,

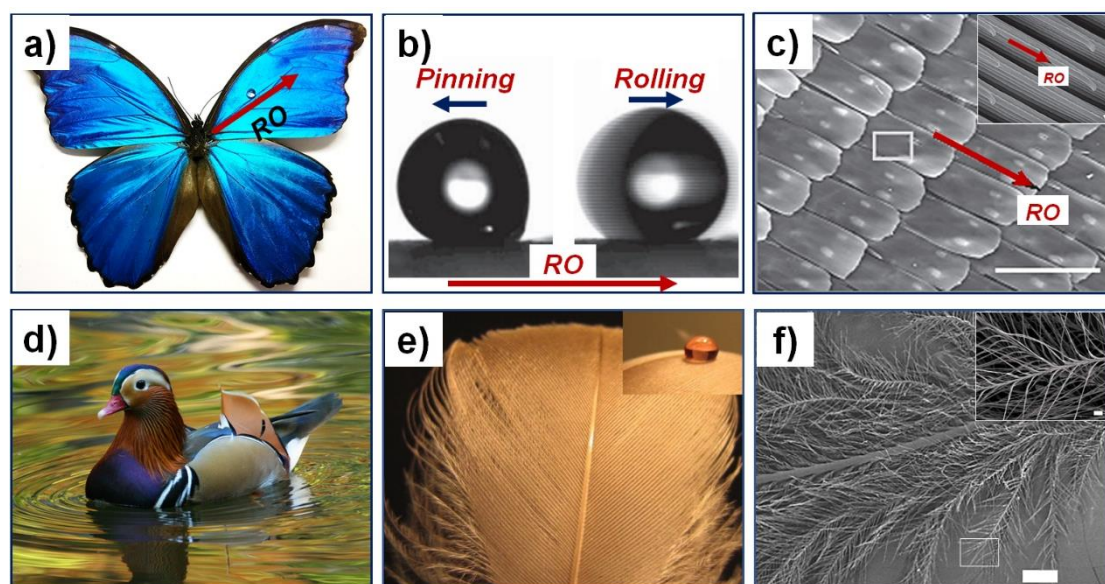


Figure 3. Nature examples with unidirectional droplet movement. a) An iridescent blue butterfly *M. aega*. The black arrows denote the radial outward (RO) direction away from the body's centre-axis. b) The water droplet was pinned on the wings with the scale tilted and adhered to the rear of the drop when N_2 airflow was blew against the RO direction, while, the droplet easily rolled off the surface as N_2 airflow was blew against the RO direction. Copyright © The royal society of Chemistry 2007. c) Hierarchical micro/nano structures on the surface of the wings. Copyright © The royal society of Chemistry 2007. d) Optical images of duck (*Anatidae*). Copyright © Baidu Baike. e) Optical image of a piece of duck feather and a water droplet on a duck feather (inert picture). Copyright © 2008 IOP Publishing Ltd. f) Multi-scale structures of duck feathers. Copyright © 2008 IOP Publishing Ltd. Scale bars: c) 100 μm , inert image: 10 nm. f) 100 μm , inert image: 10 μm .

but will be pinned against the RO direction (**Figure 3a** and **3b**, Zheng et al. 2007.). To uncover the underlying mechanism of this phenomenon, the authors carefully investigated the detailed structures of butterfly wings. As shown in **Figure 3c**, with a length of $\sim 150 \mu\text{m}$ and a width of $\sim 70 \mu\text{m}$, lots of quadrate scales have cover the superhydrophobic wings of butterfly, which also develop into a periodic hierarchy along the RO direction by overlapping each other. The inserted images in Figure 3c demonstrated the quadrate scales were also composed of numerous separate ridging stripes of $184.3 \pm 9.1 \text{ nm}$ in width and $585.5 \pm 16.3 \text{ nm}$ in clearance on the surface of each scale. This flexible micro/nano structures will result in different contact modes of a droplet, that is discontinuous three-phase (solid/liquid/gas) contact line (TCL) along RO direction while quasi-continuous TCL against RO direction, which will produce low adhesive force along RO direction and large adhesive forces against RO direction. This elegant finding opened an avenue to applying in easy-cleaning coatings. For example, in

2011, Mei et al. found that the superhydrophobic butterfly wings could effectively retard low-temperature-induced wetting, and achieve water repellence, accompanied with low adhesion under environmental humidity conditions, which show potential applications in anti-frosting, anti-fogging and anti-icing projects (Mei et al., 2011).

The phenomenon of directional droplet movement on superhydrophobic surfaces can be also observed on feathers (**Figure 3d**). In 1970, Kennedy reported that water droplets on feathers tend to roll off distally through measuring the angle of tilt required to roll drops of water (Kennedy 1970). Kennedy supposed that when drop moves distally off the feather, it will press down the distal barbules in its path; however, as it moves proximally, the barbules rise up against it. The strong water repellence of feather is mainly attributed to their porous structures and grease coating on feather surfaces (**Figure 3e**, Zhang et al. 2008). In 2013, Liu et al. carefully investigated the non-wetting phenomena of duck feathers (Liu et al. 2013).

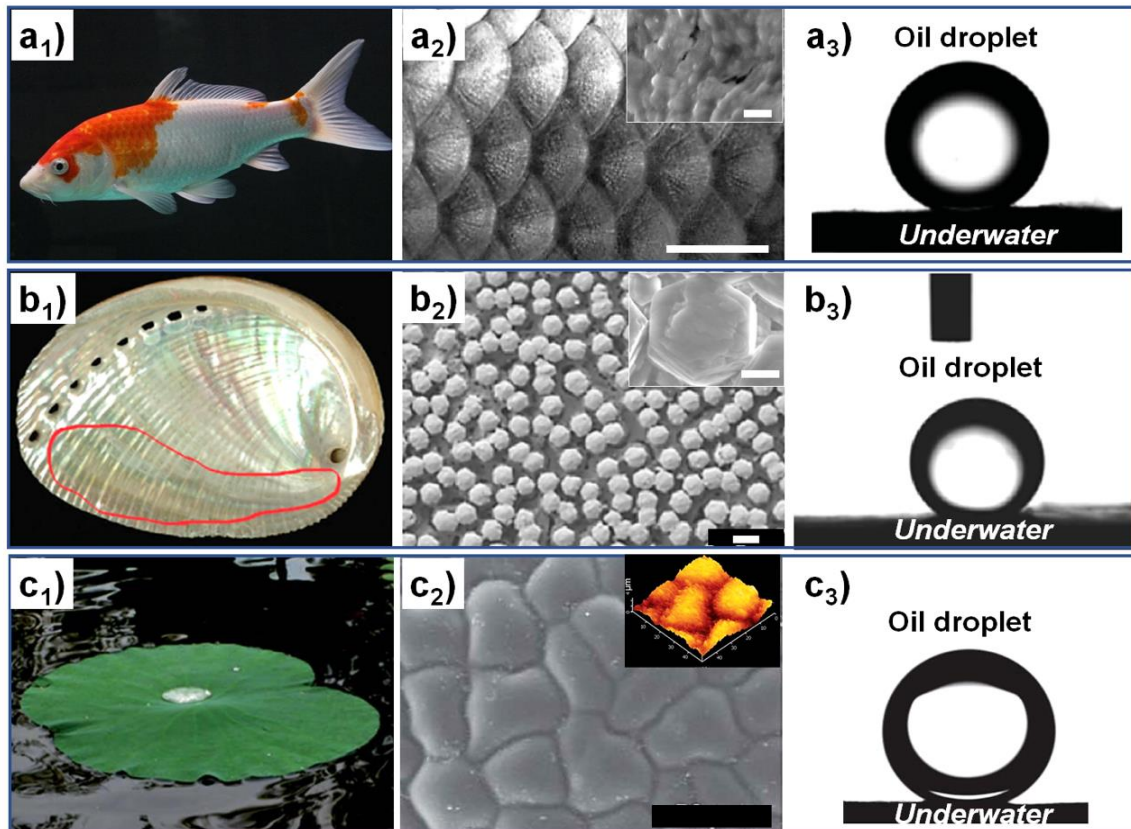


Figure 4. Underwater superoleophobicity has been discovered and inspired by underwater organisms. a) Fish scales showing the superoleophobicity underwater. (Liu et al. 2009). Copyright © 2009 WILEY-VCH Verlag GmbH & Co. KGaA, Weinheim. a₁. Optical image of fish in the water. a₂. Optical image of the fish scales. The sector-like scales with diameters of 4–5 mm arrange into an array. Inserted SEM image of fish scale showing the micropapillae. Nanostructures can be observed on the papillae. a₃. Oil contact angle on a fish-scale surface. e) Oil droplet adhesive-force measurement process on micro/nanostructured silicon substrates. b) The inner side of Columnar Nacre showing superoleophobicity underwater. Copyright © 2016 WILEY-VCH Verlag GmbH & Co. KGaA, Weinheim. b₁. Photograph of the entire abalone shell. b₂. Top-view SEM images of the inner nacreous layer in the red marked area of Figure b₁, showing convex hexagonal microscale columns and nanoscale protrusions. b₃. Photograph of an underwater oil droplet on the red marked region, with a contact angle of $156.8 \pm 0.9^\circ$. c) Lower surface of lotus leaf showing superoleophobicity. Copyright © 2011 The Royal Society of Chemistry. c₁. Picture of lotus leaf floating on the water surface. c₂. The Environment scanning electron microscope (ESEM) image shows that the lower side of the leaf consists of numerous tabular and slightly convex papillae with 30–50 mm length and 10–30 mm width. The inserted image is the Atomic force microscope (AFM) image that further shows the tabular papillae are covered with nanogroove structures with size of 200–500 nm and the height of a single papilla is around 4 mm. c₃. An oil droplet on the lower surface of the lotus leaf with a contact angle of $155.0 \pm 1.5^\circ$.

As shown in **Figure 3f**, the duck feathers are composed of branches with different dimensions, including micro-sized backbones, trunks and barbules, which facilitate the feather with porous structures. The porous structures as well as the grease with low surface tension will endow the feathers with a large air-water interface, i.e., large air proportion, contributing to distinguished water repellence (Liu et al., 2013).

2.2. Other nature-inspired self-

cleaning mechanisms

2.2.1. Underwater-superoleophobic-based self-cleaning mechanism

Oily wastewater and spilled oil are great threats for seabirds, whose feathers are usually hydrophobic and easily wetted by oils, while fish can swim in oil-polluted water and keep their body clean (**Figure 4a₁**). In 2009, Liu et al. uncovered the underlying mechanism of fish scales repelling oils and developed a novel strategy in designing

superoleophobic interfaces without the assistance of fluorinated compounds (Liu et al., 2009). As shown in **Figure 4a2**, the sector-like fish scales have diameters of 4-5 mm. To adapt to the water environment, the fish scales are hydrophilic and composed of calcium phosphate, a protein, and of a thin layer of mucus. Fine-scale roughness can be observed on micropapillae by high-magnification SEM images, which plays a key role in the superoleophobic property in water (the inserted picture in **Figure 4a2**). Oil (e.g., 1,2-dichloroethane) contact angle on the fish scale is $156.4 \pm 3.1^\circ$, which showed its superoleophobic properties (**Figure 4a3**). Inspired by fish scales, Liu et al. have prepared a superoleophobic silicon surface with micro/nano structures, on which the shape of oil drop was spherical during the whole measurement. The adhesive force was smaller than $1 \mu\text{N}$, and the oil drop could be transferred away without losses. The authors also schematically illustrated the superoleophobic wetting state. In such a case, water molecules can be trapped in the micro/nano structures, which prevents oil molecules from contacting with the solid surface. These experiments demonstrated that the micro/nano structures and hydrophilic wettability plays a key role in obtaining superoleophobic properties. In addition to fish scales, shark skin (*Isurus Oxyrinchus*) and pilot whale (*Globicephala melas*) skin, with unique structures and superhydrophilic wettability, not only anti-fouling but also enable them to swim faster and more efficiently (Ball, 1999; Baum et al., 2002). Inspired by these underwater organisms, Xue et al. have prepared a novel underwater superoleophobic polydivinylbenzene (PAM) hydrogel-coated mesh, which selectively separates water from oil/water mixtures with a high separation efficiency and resistance to oil fouling (Xue et al., 2011). In 2014, Cai et al. revealed the unique anisotropic underwater oleophobicity of filefish skin (*Navodon septentrionalis*), which is attributed to the anisotropic microtextures on the surface and hydrophilic surface composition (Cai et al. 2014).

Besides the fish skin, in 2016, Guo *et al.* also reported natural columnar nacre from abalone shell illustrating outstanding underwater superoleophobicity with excellent mechanical properties (**Figure 4b1**). As shown in **Figure 4b2**, the inner surface of natural columnar with an iridescent colour has many convex hexagonal columnar structures, of which the average side length is $\sim 3 \mu\text{m}$ and adjacent distance is irregular and $\sim 3 \mu\text{m}$. The top surface of hexagonal columns is not flat and is composed of nanoscale aragonite particle protrusions (the inserted image in **Figure 4b2**). This combination of hierarchical micro-/nanometer structure and hydrophilic components results in underwater low adhesive superoleophobicity. The contact angle of underwater 1, 2-dichloroethane droplets on the surface of columnar nacre is as high as $156.8 \pm 0.9^\circ$ (**Figure 4b3**). Inspired by natural columnar nacre, the same authors constructed layered montmorillonite/hydroxyethyl cellulose (MMT/HEC) artificial nacre-like materials, illustrating high contact angles of various oils (higher than 156.8°) and ultralow underwater oil adhesion (less than $3.5 \mu\text{N}$ against various oils) (Guo et al., 2016).

As a well-known example of superhydrophobicity, the upper side of a lotus leaf can make the water freely roll off resulting in the “Lotus effect”. Compared with the upper side of the leaf, the wettability of its lower surface raised less interest. However, after additional research effort, the importance of the wettability of the lower surface was gradually uncovered. In 2011, Cheng et al. revealed that the lotus leaf shows Janus property, i.e. that its lower surface is superhydrophilic in air and superoleophobic under water (**Figure 4c1**, Cheng et al.) As shown in **Figure 4c2**, the lower side of lotus leaf is composed of numerous tabular and slightly convex papillae with a 30-50 mm length and a 10-30 mm width. The inserted image in **Figure 4c2** was obtained by atomic force microscope (AFM), which shows that the papilla is covered with nanogroove structures with the size of 200-500 nm and

the height of a single papilla is around 4 nm. The authors also tested the underwater contact angle of various oils, including 1,2-dichloroethane, n-hexane, rapeseed oil, sunflower oil and octanol, on the lower side of a lotus leaf. As shown in Figure 4c2, taking 1,2-dichloroethane as an example, the oil contact angle (OCA) reaches up to $155.0 \pm 1.5^\circ$ which illustrates its underwater superoleophobicity. These natural examples with underwater-superoleophobic-based self-cleaning properties will hopefully offer new insights to the design of functional interfaces in marine antifouling, microfluidic devices, resistance reduction for oil transportation, oil/water separation, etc.

2.2.2. Slippery-based self-cleaning mechanism

In 2011, a new type of self-cleaning surface named as slippery liquid-infused porous surface (SLIPS) was invented, inspired by *Nepenthes Alata* (Wong et al., 2011; Lafuma and Qu  e 2011; Smith et al.,

2013; Xiao et al., 2013; Cao et al., 2015). As shown in Figure 5a and b, the peristome of this plant, of which micro/nano structures are immersed by water or nectar developing into lubricant layer, shows exceptional low friction force to insects (Bohn and Federle, 2004; Chen et al., 2016). SLIPS employed the same mechanism with lubrication liquid held in the texture of the surface. The lubrication liquid introduces a new phase between the solid surface and the foreign phase (Figure 5c). Inspired by the pitcher plant, Wong et al. prepared SLPS surface by infusing low-surface-tension perfluorinated liquids into porous/textured solid (Figure 5d). Owing to the molecular smoothness and defect-free of the low surface energy liquid fixed on the surface, the SLIPS exhibits extreme liquid repellence, *i.e.*, very low contact angle hysteresis and very low sliding angles, against various liquids of surface tension, e.g., *n*-pentane ($\sim 17.2 \pm 0.5$ mN/m) (Figure 5e).

Notably, the stability of lubrication liquid causes some concerns. The lubrication liquid

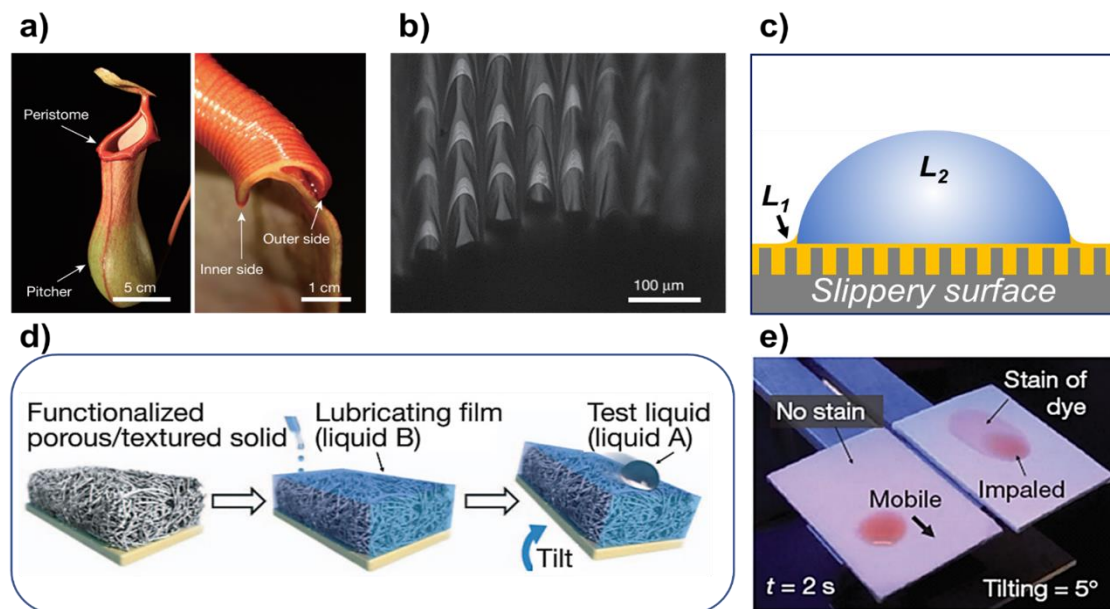


Figure 5. An emerging type of self-cleaning surfaces inspired by *Nepenthes* pitcher. a, b) Optical images of *Nepenthes Alata* and Microstructure surface from the *Nepenthes Alata*. The microchannel structures with arch-shaped cavities effectively guide the liquid flowing (Chen et al. 2016). Copyright   2016, Macmillan Publishers Limited. c) The mechanism under the slippery surface. The surface energy is controlled by the mediated liquid (L_1) irrespective of the solid surface underneath, as there is no direct contact between the test liquid and the solid surface. d) The prototype of slippery liquid-infused porous surface (SLIPS) inspired by *Nepenthes* pitcher. e) The self-cleaning properties of SLIPS (left side in the image) compared to superhydrophobic surfaces (right side in the image). The test liquid is dyed Pentane and the test clearly shows the Pentane drop can be mobile on the SLIPS without a trace (Wong et al. 2011). Copyright   2011, Macmillan Publishers Limited.

would be gradually diminished as parts of the liquid phase were to be taken with a foreign phase when slipping away or the evaporation effect exposed to the open air. More efforts were made to increase the stability of the lubrication liquid layer by employing a variety of surface chemistries, surface structures and materials, which develop this new type of surfaces. Self-replenishing SLIPS was fabricated to compensate for the loss of the lubrication liquid. The methodology comprises locating lubrication liquid inside the solid phase to create a reservoir to supply the losing lubrication on the solid surface, which keeps the lubrication property on the surface without any other coating or replenishing process (Zhao et al., 2018). The solid lubrication could be capable of resolving the complexity of the liquid lubrication.

2.2.3. Gecko-foot-inspired dry self-cleaning mechanism

As an amazing animal with an excellent adhesive force, the gecko has been found to “run up and down a tree in any way, even

with the head downwards” by the ancient Greek philosopher Aristotle in the fourth century BC (Autumn et al., 2002; Liu et al., 2012). **Figure 6a** shows a tokay gecko that can cling to vertically placed transparent glass and support its body mass (Hansen et al., 2005). In 2000, for the first time, Autumn et al. directly measured a single setal force using a two-dimensional micro-electromechanical systems force sensor and a wire as force gauge (Autumn et al., 2000). A single seta can generate up to 200 μN of force, which can even hold the mass of a small ant. As shown in **Figure 6b ~ d**, the gecko footpad is covered by millions of well-aligned fine microscopic setae of the sizes of approximately 110 μm in length and 5 μm in diameter. The micro-sized setae are split into hundreds of smaller nanoscale ends called spatulae, with the sizes of 200 nm ~ 500 nm (**Figure 6e**). The van der Waals forces generated by millions of gecko spatulae are believed to be the source of the adhesive force that allows geckos to climb vertical walls or across ceilings. The van der Waals mechanism implies that the gecko adhesion depends more on surface geometry than on

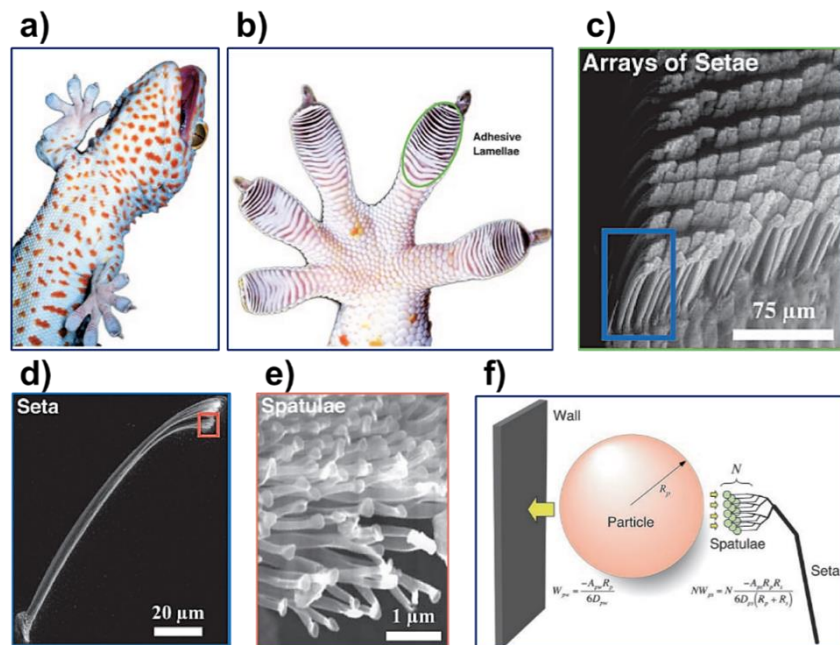


Figure 6. Gecko’s dry adhesive system (Hansen and Autumn, 2005). Copyright © 2015, National Academy of Sciences. a) Optical image of a tokay gecko climbing vertical transparent glass. b) Optical image of Gecko’s foot, which is endowed with adhesive lamellae as overlapping pads. c) SEM image of setae arrays on Gecko’s foot. d) SEM image of the proximal portion of a single lamella taken from setae arrays. e) single seta with branched structure at upper right, terminating in hundreds of spatula tips. f) Model of interactions between N (number of particle-spatula interactions) gecko spatulae of radius R_s , a spherical dirt particle of radius R_p , and a planar wall.

surface chemistry. Inspired by geckos, in 2003, Geim et al. reported a novel “gecko tape” prepared by microfabrication of dense arrays of flexible plastic pillars, whose geometry was carefully designed to ensure their collective adhesion and self-cleaning property (Geim et al., 2003). After uncovering the secret of Gecko cling on the ceiling, there is a new question arising of how the Geckos can keep their foot clean with huge adhesive forces. This type of self-cleaning was defined as dry self-cleaning. In 2005, Hansen et al. reported that Tokay gecko feet contaminated with dirt particles can be capable of recovering their ability to cling to vertical surfaces after only a few steps on clean glass (Hansen and Autumn, 2005). They have built a contact mechanical model to show that the energetic non-equilibrium between the dirt particle adhering on substrate or spatula results in the self-cleaning phenomenon (**Figure 6f**). The interaction energy between a spherical dirt particle and a planar wall can be deduced as

$$W_{pw} = \frac{-A_{pw}R_p}{6D_{pw}} \quad (1)$$

where p and w are particle and wall, respectively; A is the Hamaker constant (typically $\sim 10^{-19}$ J for van der Waals interactions in air); and D is the particle-to-wall distance (Israelachvili, 1992). The interaction energy between a spherical dirt particle and a spatula (s) is presented by the following equation:

$$W_{ps} = \frac{-A_{ps}R_pR_s}{6D_{pw}(R_p + R_s)} \quad (2)$$

N refers to the number of particle-spatula interactions needed to achieve energetic equilibrium with particle-wall interaction. If less than N spatulae are attached to each particle, self-cleaning will happen as a consequence of energetic disequilibrium, i.e. a particle-substrate adhesive force (F_{pw}) overcomes the seta-particle adhesive forces (F_{ps}), or simply F_{pw} is larger than F_{ps} . In addition, based on this model, it can be learned that setal self-cleaning strongly depends on the particle and spatula sizes and spatula material properties (e.g., low surface energy is beneficial for self-cleaning).

Although Hansen et al. revealed how geckos managed to keep their feet clean while walking with sticky toes, this model could not give a complete explanation of why certain particles demonstrate a preference to bind more strongly to the toe pads than to the substrate surfaces. In 2008, Lee et al. were first to prepare gecko-like polypropylene microfibrillar adhesive with self-cleaning properties (Lee and Fearing, 2008), which demonstrated that the shaking of the particles during the shearing process resulted in that seta arrays shed most of the particles. In 2012, Hu et al. tested the self-cleaning of geckos during locomotion, which illustrated that geckos clean their feet through a unique dynamic self-cleaning mechanism via unique digital hyperextension process (Hu et al., 2012). When the setae suddenly release from the attached substrate, a significant inertial force, i.e. the cleaning force, will be generated to dislodge the dirt particles from the attached spatulae. In 2014, based on their experimental results and theoretical models, Mengüç et al. proposed that the dominant mechanism of contact self-cleaning is particle rolling during the drag process and they suggested that the dragging rate and average load are two critical parameters that affect the performance of the self-cleaning process (Mengüç et al., 2014). In 2015, Xu et al. fabricated artificial setae using synthetic polyester microfibers (10 mm in diameter) that are cut to form a micro-pad at its tip and bonded to an AFM cantilever (Xu et al., 2015). Using the latter device, the authors measured a single artificial gecko seta and spatula F_{pw} and F_{ps} in different shearing and pull-off velocities, with the results revealing that the particle-wall adhesion is velocity dependent, whereas spatula-particle adhesion is not. These explorations in uncovering the underlying mechanisms of dry self-cleaning of Gecko will open new approaches for micromanipulation of particles, which can find wide applications in microelectromechanical systems, biomedical devices, and so on.

3. Numerical modelling of self-

cleaning mechanisms

3.1. Numerical modelling of self-cleaning on superhydrophobic surfaces

There have been numerous numerical studies in which the complex behaviour of water droplets on superhydrophobic surfaces is investigated. It is in the same time noteworthy that a similar effort is entirely missing when it comes to including contaminants - solid particles - of different surface properties (i.e. wettabilities) and shapes and formulating a comprehensive particle-droplet-superhydrophobic surface numerical framework. In other words, numerical studies in this field have so far focused on explaining the conditions and the involved relevant phenomena that would make possible the process of self-cleaning on a certain superhydrophobic surface. For the latter purpose, different numerical frameworks were used (phase-field-method in (Liu et al., 2014), Volume of Fluid (VOF) method in (Attarzadeh and Dolatabadi, 2017) and Lattice Boltzmann method in (Wang et al., 2017) to resolve a set of events that lead to jumping of the resulting droplet and the subsequent possible removal of a contaminant. In general, attention was paid to modelling of the contact angle of the droplet (needed for calculating the adhesive force between the droplet and the surface) and to the investigation of the importance of possible pockets of trapped air between the droplet and the asperities of the surface. Studies typically test a number of configurations of the superhydrophobic surface, for example the use of a series of micro-patterned pillars or nano tubes. The goal is to obtain a structural characterization of self-cleaning surfaces and thus recommendations for their future design through a systematic variation of measures for achieving and promoting the self-cleaning process.

3.1.1. Lotus effect

The research effort related to self-cleaning has so far focused on two major areas: i)

design and fabrication of self-cleaning surfaces, typically in the form of biomimetic nanostructures in which inspiration from nature is sought to produce the desired structuring of surfaces and their chemical functionalization, and ii) understanding of various mechanisms of self-cleaning and of specific phenomena related to, for example, behaviour of droplets on different surfaces. Even if the recent years have seen a significant advance in the field, a breakthrough is yet to come in being able to fully resolve the multifaceted physics of the process. In both types of obstacles, numerical simulations can be of great help contributing to both understanding fundamental physical phenomena and designing enhanced-performance surfaces for industrial applications.

Although self-cleaning is possible on hydrophilic surfaces, we will focus here on superhydrophobic ones. Superhydrophobicity of a surface, caused by a combination of surface roughness and low-surface-energy coating, facilitates the desired self-cleaning effect. A major role in the process is played by the condensed water droplets that remove contaminants from a surface through two major mechanisms: the first one is removal by rolling droplets, in which the droplet crawls over the particle, collects it and takes it away. This is the previously discussed "Lotus effect" that always implies presence of external forces, such as gravity. The existence of distinctive microscopic structural and chemical properties on reptiles, plants or insects (Blossey, 2011; Barthlott and Neinhuis, 1997) and connected to the self-cleaning process has led to the principle of "biomimetics", where the self-cleaning features in technological applications are achieved by mimicking the micro- or nano-structures on the identified examples from nature. Self-cleaning surfaces in nature typically involve rain or condensed water droplets, have to be tilted and require the action of gravity to remove contaminants. The main principle behind the "Lotus effect" removal of contaminants is shown in Figure 1e and f.

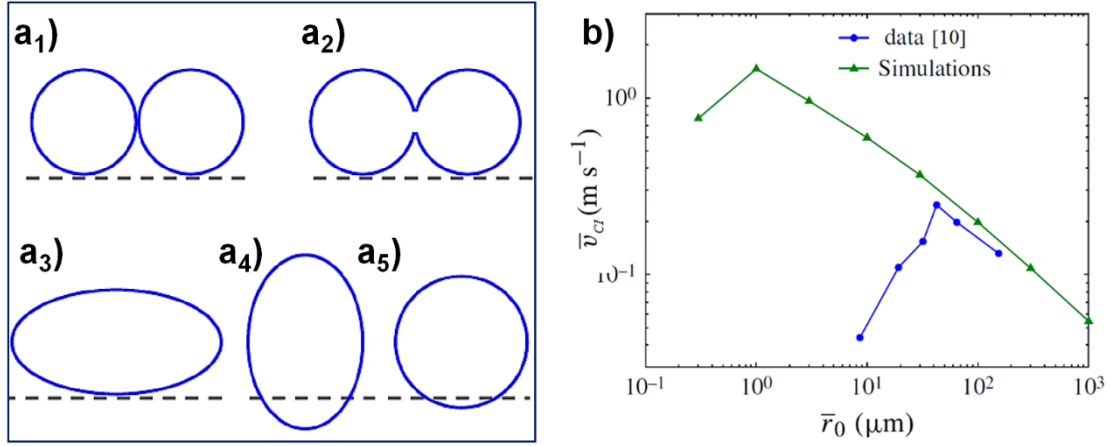


Figure 7. a) Mechanisms of jumping of a droplet from a surface (Liu et al. 2014). Copyright © 2014, Cambridge University Press. The dashed line gives the position of an imaginary substrate. Its actual presence would break the symmetry of the oscillations and the resulting spherical drop would jump off the surface. b) Validity of capillary-inertial (CI) scaling- comparison between numerical simulations (Liu et al., 2014) and experimental data taken from (Boreyko et al., 2009). Copyright © 2014, Cambridge University Press. The power law is indicated by a diagonal line in the logarithmic graph. Note the significant difference between the cut-off lengths predicted by the simulations (0.3 μm) and the experiments (30 μm). The difference exemplifies the crucial importance of including the full resolution of drop-surface adhesion in the simulations.

Furthermore, the same figure schematically illustrates why superhydrophobic surfaces are needed to facilitate self-cleaning. We see that contaminants are only redistributed by water on smooth surfaces, whereas on rough surfaces they adhere to the droplets surfaces and are thereby removed from the leaves when the droplets roll off.

In summary, there are several fundamental principles that we can learn from nature and then use in technological applications: i) the surface is hydrophobic or superhydrophobic (there is a degree of roughness that minimizes the contaminant-droplet interface and enables a high contact angle), ii) the droplet is spherical on such a surface, which will facilitate rolling off droplets together with the collected particles instead of just water crawling over the particles and iii) gravity is needed to remove the droplet and the particles from the surface. This method can thus be termed “the rolling mechanism” of self-cleaning.

3.1.2. Droplet jumping effect

Numerical studies can reveal a great deal about the dynamics and the overall role that droplets play in the process of self-cleaning. For example, valuable information can be

obtained about the mechanisms of jumping, even without the presence of any substrate. **Figure 7a** (Liu et al., 2014) starts with two identical adjacent droplets (**Figure 7a**), continues with formation of a liquid bridge between them upon initiation of coalescence (**Figure 7b**), then with several cycles of the so-called capillary-inertial (CI) oscillations between oblate and prolate shapes of the merged drop (**Figures 7c** and **7d**), until the merged drop finally takes a spherical shape due to viscous dissipation.

Furthermore, it is accepted that the jumping process is governed by the capillary-inertial (CI) jumping speed $v_{ci} \sim \sqrt{\frac{\sigma}{\rho r_0}}$, and the

CI timescale is $t_{ci} \sim \sqrt{\frac{\rho r_0^3}{\sigma}}$ (in sub ms), with σ being the surface tension, ρ liquid density and r_0 the initial drop radius. Note that, in reality, the true jumping velocity is only a part of the CI velocity, which means that only a fraction of the excess free energy is convertible to the useful kinetic energy, available for jumping. This implies that a relatively large power density is needed to achieve self-cleaning. The validity of a $v_{ci} \sim r_0^{-1/2}$ scaling has been checked by numerical simulations (Liu et al., 2014).

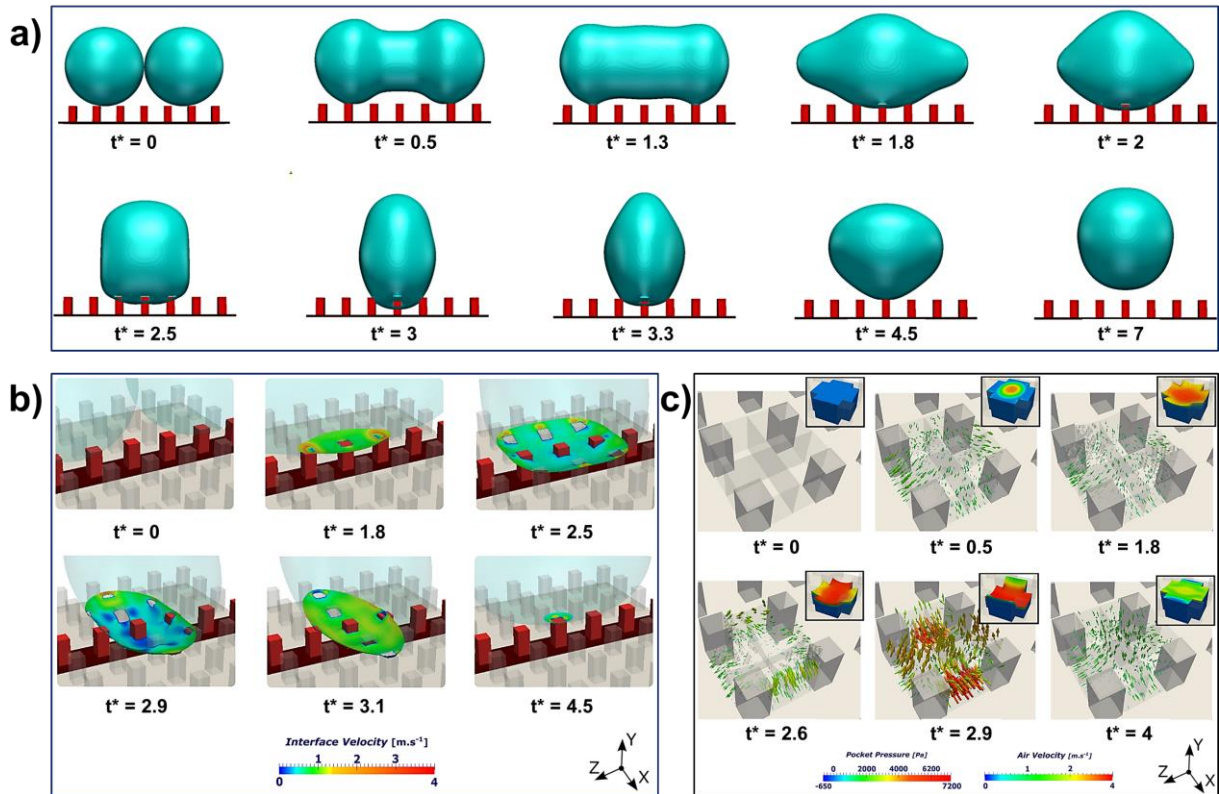


Figure 8. Numerical simulations of coalescence-induced jumping of micro-droplets on heterogeneous superhydrophobic surfaces (Attarzadeh and Dolatabadi, 2017). Copyright © 2017, AIP Publishing. a) Coalescence of two micro drops-jumping on a superhydrophobic surface. The surface is represented as a series of micropillars. b) Evolution of the droplet interface inside the cavities of a superhydrophobic substrate. The figure starts with a coalescence of two identical microdroplets (radius 20 μm). c) Dynamics of air during coalescence of microdroplets. The figure shows both air velocity vectors at various instances and interface pressure on the upper surface of the air pocket.

Figure 7b shows the mentioned power law as a line parallel to a diagonal line of the logarithmic graph, as obtained from simulations (Liu et al., 2014) and experiments (Boreyko et al., 2009). We see that there is a two-orders-of-magnitude difference between the two in predicting the viscous cut-off radius below which the CI scaling will not hold. The difference is in (Liu et al., 2014) attributed to not taking into account the drop-surface adhesion, which in turn rendered the complex drop-surface interaction erroneously represented.

It has been suggested in (Miljkovic et al., 2013) that the internal fluid dynamics of droplets during the coalescence process determine the fraction of the excess surface energy that will convert into the kinetic energy of jumping motion. The jumping of a droplet then comes from the counter action of the rough surface to the impingement of the

liquid bridge between the coalescing drops. The obtained kinetic energy has to overcome the adverse forces (adverse to jumping), such as gravity and vapour flow. Numerical simulations are able to successfully reproduce this entire process (Attarzadeh and Dolatabadi, 2017). **Figure 8a** also exemplifies taking into account a superhydrophobic nature of the surface by modelling protrusions as a series of micropillars.

Numerical simulations are carried out with such resolution that they straightforwardly capture the complex interactions between a droplet resulting from coalescence of microdroplets and microstructure of a superhydrophobic substrate. One such example is from (Attarzadeh and Dolatabadi, 2017) where the evolution of a fraction of the droplet interface between the strip of micropillars is shown. **Figure 8b** shows the

liquid interface underneath the droplet, which presents the penetration of the droplet inside the cavities of the substrate.

In addition, significant information about the dynamics of the air underneath the microdroplet is provided by the simulations. Changes in the geometry of the air pocket follow the process shown in Figures 8 and 9. **Figure 8c** (Attarzadeh and Dolatabadi, 2017) gives the evolution of the upper surface of the pocket as subjected to the curvature of the microdroplet (insets in all subfigures in Figure 8c). The pressure changes as the droplet penetrates the cavities and thus pressurizes the air. The same figure nicely exemplifies the necessity to resolve all steps in the process in Figure 8c-among others resolution of the liquid bridge between the micro droplets in the beginning of the process. We see that in the first three subfigures of Figure 8c the outward motion of the air through passages is observed as the liquid bridge is forming.

An important question in a mechanism of self-cleaning without the presence of external forces is the estimation of the energy available for jumping to take place. **Figure 9** (Liu et al., 2014) gives the energy budget during the process and shows that the total energy of the merged drop can be represented as a sum of the surface and kinetic energies and also that it decays over time due to

viscous dissipation. Furthermore, the kinetic energy of the merged drop can be decomposed into translational and oscillatory parts (Figure 9, bottom). Since the latter part of the total kinetic energy does not contribute to any net motion (it becomes dissipated eventually), the goal of any design of a superhydrophobic substrate with the purpose of self-cleaning should aim at minimizing the oscillation component.

The relative importance of a number of parameters (inertia, viscosity and the density ratio between the phases) in the jumping of the merged droplet was numerically investigated in (Farokhirad et al., 2015). It was found that the surface wettability (i.e. the contact angle when the droplet jumps away from the substrate) did not depend on the density ratio. In addition, the same study showed that for contact angles greater than 150° there exist two different dynamical regimes for different density ratios, identified as inertial and viscous regimes. In (Wang et al. 2017) the authors looked at the coalescence of droplets of different sizes. The study identified a critical droplet ratio below which the jumping of the merged droplet did not take place. The influence of coalescence of three or more droplets and their initial position on the jumping process was numerically investigated in (Wang et al. 2017). The coalescence behaviour was

classified into two types: the one termed “concentrated configuration” in which all droplets coalesce instantaneously, and the other labelled “spaced configuration”, where two drops first merge and then sweep up the third one in its moving path.

In summary, the available level of information of the present numerical studies when investigating the process of self-cleaning provides valuable

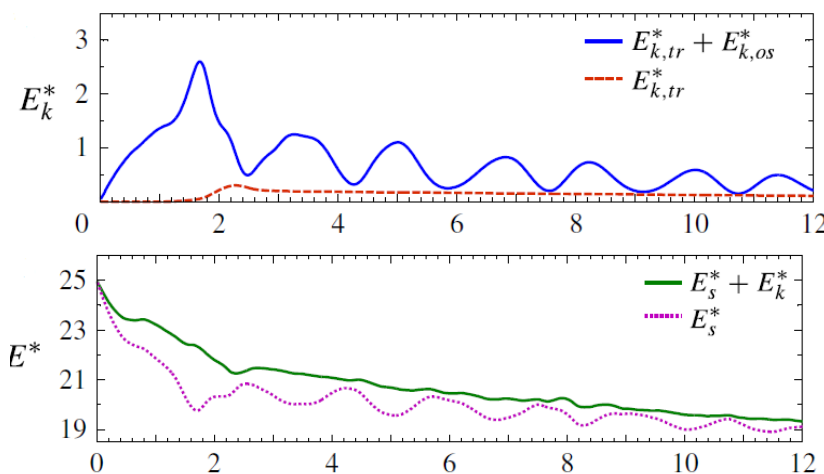


Figure 9. Top: total energy (surface and kinetic) of the merged drop vs. non-dimensional time during the jumping process. Bottom: the kinetic energy as a sum of translational and oscillational energies (Attarzadeh and Dolatabadi, 2017). Copyright © 2017, AIP Publishing.

information for design and development of self-cleaning surfaces in a variety of applications and maximization of the self-cleaning effect. In combination with experiments, it is to be expected that the simulations will provide recommendations for design and fabrication of self-cleaning surfaces through a systematic variation of measures for achieving and promoting the self-cleaning process.

3.2. Numerical modelling of self-cleaning on *superoleophobic* surfaces

In this section we will look at specific features of numerical modelling of self-cleaning on *superoleophobic* surfaces and in relation to the mechanisms of self-cleaning identified above (self-propelled jumping droplets). Although the issue of terminology in this field is far from generally accepted (Marmur, 2012), we define here a surface *superoleophobic* if it displays the apparent contact angle larger than 150° (the same conditions as with *superhydrophobic* surfaces) and if the working liquid has a low surface tension. Furthermore, we accept a common name of *superomniphobic* surfaces for both *superhydrophobic* and *superoleophobic* surfaces, i.e. for surfaces that are extremely water repellent to both high surface tension liquids (e.g. water) and low surface tension liquids (e.g. oils and alcohols). We will thus discuss in this section whether the latest advances in numerical modelling related to *superoleophobic* surfaces can match the same efficiency of the discussed self-cleaning mechanisms as that on *superhydrophobic* surfaces.

We have seen in the previous Section that the efficiency of converting the excess surface energy of the coalescing droplets into the kinetic energy of jumping can be very low even for *superhydrophobic* surfaces (i.e. when high surface-tension fluids are used). The problem is far more pronounced on *superoleophobic* ones (due to the lack of sufficient excess surface energy) and, until recently, very little effort has been invested in using numerical simulations to identify the

ways to increase this efficiency. We recall here that, in terms of fluid mechanics, the self-propulsion of droplets on super-repellent surfaces is closely related to the scaling of the non-dimensional jumping velocity (v^*) with the Ohnesorge number: $v^* \sim \sqrt{1 - Oh}$. Self-cleaning on *superoleophobic* surfaces is expected to belong to the so-called visco-capillary regime (high Oh), for which the released excess surface energy can be either significantly or totally consumed by viscous dissipation. In such a case, $v^* \rightarrow 0$ and the droplet cannot jump from the surface.

In a recent work Vahabi et al. (Vahabi et al, 2017) experimentally and numerically investigated different regimes of coalescence-induced self-propulsion of droplets on *superoleophobic* surfaces. The authors systematically varied droplet radii, viscosities and surface tensions (including very low surface-tension liquids) of the interacting droplets. A numerical part of the study was carried out using a VOF numerical framework. An important result is a map of regimes on a *superoleophobic* surface, which demarcates an inertial-capillary- from a visco-capillary regime and also gives the value of Oh (~ 0.4) for which the non-dimensional jumping velocity tends to zero and the coalesced droplet no longer jumps from the surface.

The same authors (Vahabi et al., 2018) numerically investigated (again VOF was used as a numerical framework) how the design of a *superomniphobic* surface impacts the jumping velocity of a coalesced droplet. The authors found that the protruding macrotexture (in the form of a ridge) was able to effectively redirect the in-plane to the out-of-plane velocity vectors and thus significantly increase the energy conversion efficiency. The authors report an increase of the latter of incredible 600 % as compared to a *superomniphobic* surface without a macrostructure. **Figure 10a** illustrates the coalescence-induced jumping of low-surface tension droplets from a surface without (Figure 10a, top) and with the protruding macrotexture (Figure 10b, bottom). A substantial increase is manifested in the

jumping height in the case with the ridge present. Findings of this kind should clearly affect the design and manufacturing of surfaces in order to increase the self-cleaning effect.

The mentioned increase in the out-of-plane kinetic energy when the surface is modified is clearly demonstrated in **Figure 10b**. The figure gives evolutions of the nondimensional excess surface energy and the nondimensional upward kinetic energy in the two cases. The instruction of a protrusion unambiguously increases the useful part of the total energy for jumping (the red dashed line, top and bottom). The different colours in Figure 10b indicate three stages of coalescence identified in the process-stage I represents a negligible net upward velocity of the droplet, stage II indicates the impingement of the capillary bridge on the surface that forces the droplet to move upwards and, finally, stage III reflects the increase of the upward droplet kinetic energy due to the existence of a high-pressure region near the centre (without modification) or

close to the bottom of the droplet (with modification). The authors argue that it is the presence of a ridge that determines the possible alignment of velocity vectors, thus obstructing or encouraging the possible upward movement of the droplet.

The notion of how crucial the presence of a surface modification is on the alignment of velocity vectors and thus the outcome of the jumping process is shown in **Figure 10c**. In the top figure (no surface modification) the radially outward internal flow disturbs the alignment of velocity vectors and, consequently, impedes the upward motion of the droplet. The presence of a ridge, however, shows that at the same instant we have a high-pressure region at the bottom of the droplet that leads to alignment of velocity vectors in the vertical direction and resulting in the increase of the upward kinetic energy of motion (the red dashed line in Figure 10c, bottom).

4. Processes to manufacture self-cleaning surfaces

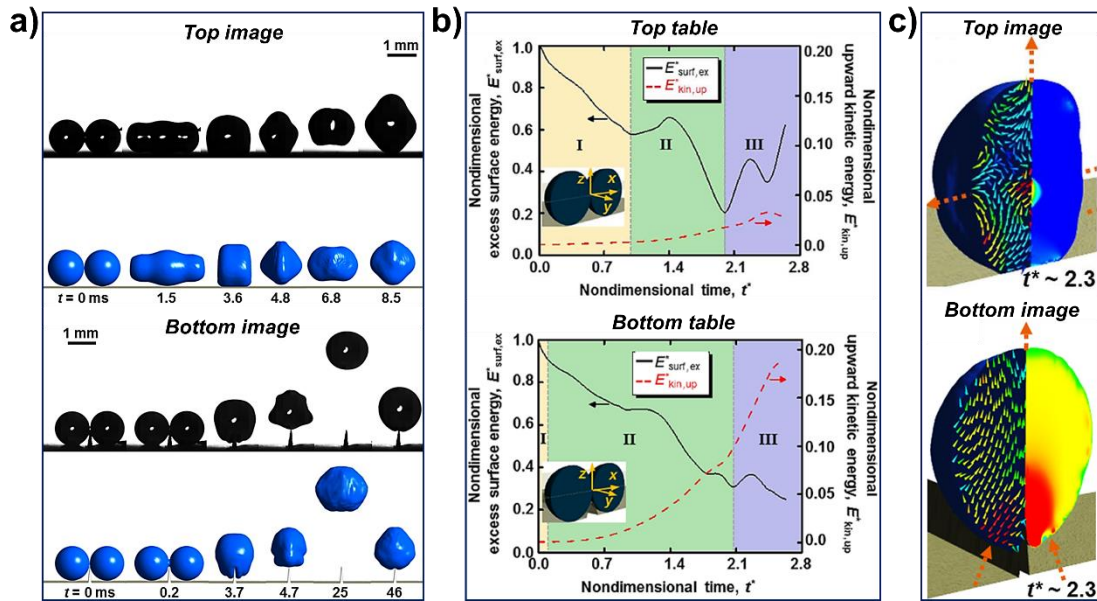


Figure 10. Coalescence-induced jumping of droplets on superomniphobic surfaces with macrotexture (Vahabi et al., 2018). Copyright © 2018, AAAS. a) Departure of the coalesced droplet from the surface with two designs of a superomniphobic surface (top: without a ridge, bottom: with a ridge). The ridge height is 500 μm . Note the difference of maximum heights of the jumping droplet in the two cases. The black cases refer to experiments, whereas the blue ones represent numerical simulations. b) Droplet dynamics without (top) and with the ridge (bottom). Note the increase in the kinetic energy of upward movement in the case with a ridge (the red dashed lines, top and bottom). The different colours indicate stages of the coalescence process. c) Different alignment of velocity vectors without (Top) and with (Bottom) the presence of surface modification as a key factor in the outcome of the jumping process. A crucial role is played by the different distribution of pressure in the two cases.

While modelling of self-cleaning mechanisms is expected to aid the understanding and design of future materials (M3 approach), it has not yet been used much for designing the materials currently used in practice. In this section, we will focus on processes for producing self-cleaning surfaces that are already on the market, with an emphasis on scalable methods, i.e., approaches that can also be applied to large surface areas. The literature describes a great number of different methods to create self-cleaning surfaces. A nice overview is given by, for example, Ganesh et al. (Ganesh et al., 2011). A significant part of their review paper is devoted to the different ways to produce hydrophobic and superhydrophobic coatings; the majority of the methods use the liquid phase. Ganesh et al. describe, for example, approaches using hydrothermal reactions, electrochemical deposition or sol-gel methods. Patterns on a surface can also be created using lithography or self-assembly, but this is not very well scalable to large areas.

A better approach might be self-assembly and layer-by-layer methods in the liquid phase. These are relatively inexpensive techniques in which micro- and nanoscale superhydrophobic structures can be fabricated with fine-controlled morphologies (Ganesh et al., 2011).

However, not all methods developed by researchers in the lab can be upscaled to a profitable process in a price-driven economy. Here we present some chosen processes that are already used to provide products biomimetic self-cleaning properties.

4.1 Self-cleaning paint

In 1999, Lotusan from Sto AG was the first paint on the market biomimicking self-cleaning surfaces. The paint was developed for substrates such as building facades. Small particles in the paint form a three-dimensional surface above the coated body (Born and Ermuth, 2005). However,

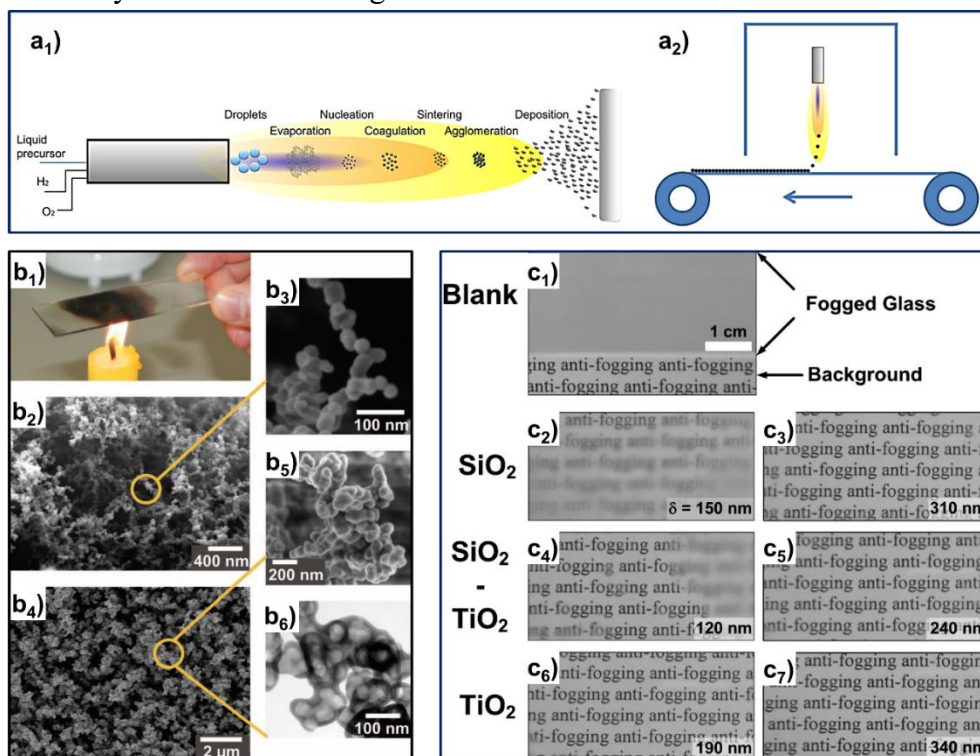


Figure 11. Liquid flame spray (LFS) coating process. a) Schematic illustration of LFS coating process (Haapanen et al. 2015). Copyright © 2015, Elsevier. a₁) Aerosol processes in LFS. a₂) Roll-to-roll coating process in LFS. b) Candle soot coating process (Deng et al. 2012). Copyright © 2012, AAAS. b₁) Optical image of depositing a soot layer on glass slide. b₂ ~ b₃) SEM images of the soot deposit. b₄ ~ b₆) SEM images of the deposit after being coated with a silica shell. c) Anti-fogging effect of various glass substrates treated by LFS (Tricoli et al.). Copyright © 2009, American Chemistry Society. c₁) Blank glass slide. c₂~ c₃) Glass slide coated by SiO₂. c₄~ c₅) Glass slide coated by SiO₂-TiO₂. c₆~ c₇) Glass slide coated by TiO₂.

nowadays dozens of similar products on the market (see e.g. Soeren et al. 2009). Another example is the paint Ultra-Ever Dry from the company UltraTech (Hasskerl, et al. 2004). The paint consists of pre-treated silica nanoparticles solved in acetone. After applying on a surface, the acetone evaporates leaving a hierarchical surface. To increase the hydrophobicity the silica nanoparticles are chemically treated in a special way. The combination of the hierarchical three-dimensional surface structures and the hydrophobic properties of the particles is clearly related to the described biological organisms. Especially to achieve the low contact angles defined as super hydrophobicity, just forming the hierarchal structures is not sufficient. Rather the combination of low surface energy materials and their structure results in the very beneficial self-cleaning properties. Therefore, the described chemical treatment of the hydrophilic silica nanoparticles is mandatory for such applications. The advantage of paints such as the described one is that processes to develop paints are known for centuries. Further, the paints can be applied on all kinds of surfaces in a simple manner.

4.2 Self-cleaning coatings by flame synthesis

Flame reactors are well known to synthesize different type of nanoparticles at very high production rates. The processes are used since decades to synthesize carbon black, titania, and silica (Zhu and Pratsinis, 1997; Stark and Pratsinis, 2002; Wegner and Pratsinis, 2003). Butt and Vollmer showed how self-cleaning surfaces can even be manufactured by using candle soot as a green body to achieve a surface showing a water contact angle of 165° (Deng et al., 2012; Vollmer et al., 2012) (see **Figure 11**). Several researchers reported how flame reactors can be used to coat different surfaces with nanoparticles to achieve self-cleaning properties, mostly using TiO_2 and SiO_2 (Teoh, et al. 2007; Tricoli, et al. 2009; Stepien et al. 2012; Salameh, et al. 2012;

Masuda and Kato, 2013; Pakdel, et al. 2013; Stepien, et al. 2015; Haapanen et al. 2015; Jesus et al. 2015).

In flame reactors, the precursor, typically in the form of a liquid, is dispersed by a gas flow under pressure and burned. Depending on the exact process, support chemicals are needed to stabilize the combustion. In the flame, nanoparticles are formed based on nucleation and coagulation. These primary particles aggregate and agglomerate leading to fractal agglomerates with a size of multiple microns (Müller, 2004; Müller et al. 2002; Müller et al. 2003). The surface to be coated is typically positioned a few tens of centimetre above or below the flame (Friedlander, 2000; Sahn et al. 2004; Sahn et al. 2007). Important is a relative movement between the flame and the surface to homogenously coat the surface. The obtained thickness of the growing layer determines the spraying time (Müller et al. 2006). The advantage of these reactors is to produce non-porous particles at high purity and with relatively narrow particle size distributions. The disadvantage of producing non-agglomerated/aggregated particles for the usual use cases turn to be a real asset for producing self-cleaning surfaces since the fragmented nature of the agglomerates automatically lead to the self-cleaning properties (Müller, 2004; Müller, 2002; Müller et al. 2003). Again, the hydrophobicity of the surfaces is significantly improved by decreasing the surface energy of the nanoparticle agglomerates by e.g. chemical treatment. Nevertheless, the stability of these layers are not very high and subsequent process steps such as sintering, mechanical compression or further surface treatments of the particles are necessary to increase the mechanical strength which is highlighted by the current research (Friedlander, 2000; Schopf et al. 2013; Nun and Schleich, 2007; Nun, 2006).

4.3 Self-cleaning coatings by sputtering

Sputtering is a physical vapour deposition method operating in vacuum where material

is removed from a target. Interestingly the research field focusing on sputtering techniques is still an active field of research, even if its beginnings date back to the 19th century. The first sputtering process was described by Grove in 1852 (Grove, 1852). In the basic sputtering process, energetic ions are generated in a glowing plasma to bombard a target. This causes the removal of target atoms which can form a thin film on top of a substrate. Further, the ion bombardment also results in the formation of secondary electrons, which are maintaining the plasma. In the past, sputtering processes were limited by low deposition rates, low ionisation efficiencies in the plasma, and high substrate temperatures (Greene, 2017). Since the late 1970s the development of magnetron sputtering made a big step towards industrial use (McLeod, 1974; Chapin, 1974). In comparison to its ancestor, magnetron sputtering is able to grow thin coatings on two-dimensional surfaces at very high production rates and with easy scalability (Greene, 2017; Bräuer, et al. 2010). While most of the other processes are operated in batch, sputtering is a continuous process. These advantages in combination with a very low price per m² makes magnetron sputtering often the favourable choice for industrial coatings.

Magnetrons use magnetic field lines to constrain the motion of the secondary electrons to the vicinity of the target. Therefore, one pole is positioned at the central axis of the target while the second pole proceeds along the outer edge of the target. The increased ionisation efficiency results in a dense plasma in the target region. This leads to increased ion bombardment of the target, giving higher sputtering rates and, higher deposition rates at the substrate. In addition, the increased ionisation efficiency achieved in magnetron mode allows the discharge to be maintained at lower operating pressure (Greene, 2017; Bräuer, et al. 2010). Based on its high industrial usage, the magnetron technique is today still continuously developed such as S-gun magnetrons (Clarke, 1977), rotatable

magnetrons (Gaertner, 2012; Price, 2012; Madocks, 2010), or magnetically unbalanced magnetrons (Ehiasarian and Munz, 2003; Renevier, et al. 2000). In literature, multiple articles describe how magnetron sputtering can be used to synthesize self-cleaning surfaces. Zeman and Takabayashi synthesized TiO₂ films via radio frequency magnetron sputtering. These films showed good self-cleaning and antifogging properties (Zeman and Takabayashi, 2002). Zhao et al. used magnetron sputtering to synthesize combined TiO₂/CeO₂ films on different glass substrates (Zhao et al., 2008). A combination of sputtering and PECVD (plasma-enhanced chemical vapour deposition) was used to create combined SiO₂/TiO₂ film with good self-cleaning properties (Chemin et al., 2018). As already reported sputtering is omnipresent when it comes to the industrial coating of e.g. glass surfaces. Especially the usage for architectural glasses, car/train glasses or solar cells boosted the development in the last decades (William et al. 2006; Azzopardi and Brasy, 2005; Gueneau, et al. 2009; Nghiem et al. 2011). While most of the work on sputtered films uses the effect of photocatalytic self-cleaning properties, some recent studies use sputtering – sometimes combined with other techniques – to obtain biomimetic self-cleaning surfaces (Xiu et al., 2006; Tulli et al., 2013; Sarkar and Pradhan, 2014; Kylián et al., 2017), e.g. by tuning the hydrophobicity.

4.4 Self-cleaning coatings by carbon nanotubes

Another way shown in **Figure 12** to mimic a nanopatterned surface can be reached by decorating a substrate with carbon nanotubes (CNTs) (Volder et al. 2013; Lau et al. 2003; Baughman et al. 2002). For high self-cleaning abilities, the synthesized nanotubes are preferably not randomly distributed over the substrate, but are rather aligned homogeneously perpendicular to the substrate. Based on this three-dimensional assembly this growing is referred as CNT forests.

Typically, such structures are grown by Chemical Vapour Deposition (CVD) (Lau et al. 2003; Kong et al. 1998; Schaffer, 2004; Grill and Singh, 2012; Lee and Lee, 2006; Zhang and Baker, 2004). In a CVD reactor, a carbon-containing precursor is decomposed at high temperature. The growth of CNTs is catalysed by the presence of metal nanoparticles such as Fe, Ni, and Co on the substrate (Yan and Miao, 2015; Su et al. 2000). The properties, yield, and quality of the CNT are strongly affected by the carbon precursor, temperature and catalyst. Methane, for example, has a high thermal stability and CVD processes are carried out above 800 °C (Yahyazadeh and Khoshandan, 2017; Kong et al. 1998; Cassell et al. 1999). However, using precursors with lower thermal stability such as ethylene or acetylene often leads to the deposition of carbonaceous compounds rather than CNTs if the process is not adequately adapted (Schaffer, 2004; Lee and Lee, 2006; Zhang and Baker, 2004). The self-cleaning properties are based on the 3-dimensional assembly. A big asset of CVD reactors is their easy upscaling. This allows a straightforward development from first lab-scale experiments to industrial production. Further, they can produce large amounts of nanotubes at high quality and competitive prices and growth rate (hundreds nm/min) (Kong et al. 1998; Cassell et al. 1999).

The small diameter of the nanotubes minimizes the contact area to water droplets and therefore is the main feature of this type of biomimetic self-cleaning surfaces. However, contact with water droplets leads to bundling nanotubes after the evaporation of the water droplet (Lau et al. 2003). Therefore, a second process step is needed to shield the tubes against this agglomeration. Advantageously, the surface energy of the nanotubes can be lowered in the same process step.

Lau et al. coated a Plasma enhanced CVD grown carbon nanotube forest with a PTFE layer (also with CVD) on a silicon substrate and showed the superhydrophobicity of such surfaces. The nanotubes had an average diameter of 60 nm and a density of 10

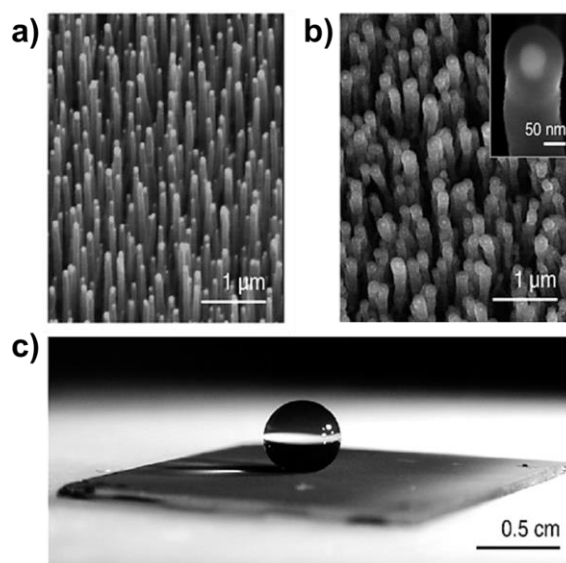


Figure 12. SEM images of carbon nanotube forests (Lau et al., 2003). Copyright © 2003, American Chemistry Society. (a) As-grown forest prepared by PECVD with nanotube diameter of 50 nm and a height of 2 μm, (b) PTFE-coated forest after HFCVD treatment, and (c) an essentially spherical water droplet suspended on the PTFE-coated forest.

nanotubes per μm² With this approach they achieved contact angles between 160-170° (Lau et al., 2003). However, such nanotube forests are not limited to flat substrates. Liu et al. used a CVD reactor to growth a nanotube forest on cotton fabrics (Zheng et al., 2007). But even more creative applications are on the market. For example, carbon nanotubes are grown onto prosthetic device to create tough skin-like self-cleaning surfaces (Simpson et al. 2012).

We can conclude that already some advanced self-cleaning materials are on the market, but it is to be expected that the recent advances in mechanistic insight and modelling will lead to further innovations in the coming years.

5. Conclusion and outlook

Surfaces have a general tendency to attract dirt when exposed to contamination, such as dust, ice or smudge. Materials in the animal and vegetable kingdom comprise a number of different strategies to avoid surface contamination. In bio-inspired materials science, researchers are taking advantage from the million years of evolution and

survival of the fittest, to learn how nature managed to cope with contamination problems. Even though such inspiration by nature is beyond doubt very useful, we have to keep in mind that nature operates using different principles than the human society. For example, biological organisms may undergo a high failure probability (i.e. fatal loss of individual plants or animals) with no critical problem for the species, as nature aims to let the species survive. In contrast, safety of each individual person is an important criterium for engineers to # develop technology, such as cars and air planes. Also, nature's materials usually undergo continuous repair processes, which can be challenging to reproduce in engineering materials (even though some limited efforts on self-healing exist). Furthermore, the lifetime of nature's self-cleaning materials, such as insect wings or plant leaves, is relatively short, such as days, weeks, sometimes months, whereas in engineering applications often lifetimes of years are demanded. Therefore, bio-inspiration is to be used prudently: it can reveal valuable new concepts, but has its limitations.

In this review, we have reviewed nature-inspired self-cleaning surfaces with a focus on mechanisms, modelling, and manufacturing (M3). We provided six kinds of nature's self-cleaning examples, i.e. the Lotus-effect (based on superhydrophobicity), insect-inspired superhydrophobic-induced droplet jumping, superhydrophobic-induced unidirectional movement of water droplets, fish-scale-inspired underwater-superoleophobic-based self-cleaning, pitcher-plant-inspired slippery-based self-cleaning, and Gecko-foot-inspired dry self-cleaning. which have been studied abundantly. As introduced above, each of these six are attributed to different self-cleaning principles, which consequently have their own advantages and disadvantages in fabrication processes as well as in applications. Among them, lotus-effect-inspired superhydrophobic surfaces can

safely be considered as the most popular, which may result from two advantages: 1) their intimate connections with practical applications ranging from anti-wetting, anti-fouling, anti-icing, oil/water separation to enhancing the efficiency of heat transfer, promoting the stability and efficiency of battery, improving the electrode efficiency in gas evolution reaction, etc. 2) because of the random micro/nano structures, which don't need to be carefully designed, their fabrication processes are relatively simple. Therefore, although we introduced six kinds of natural self-cleaning surfaces, we dedicated a relatively large proportion to the lotus-effect-inspired superhydrophobic surfaces. Huge research efforts including synthesis and modelling have already been focused on developing lotus-effect-inspired superhydrophobic surfaces. There are several commercial products to give surface self-cleaning properties. These products are highly relevant, as their application can lead to significant energy savings (preventing fouling of heat exchanger surfaces and photovoltaic panels). We have discussed three approaches that are well scalable: paint, coatings made by flame synthesis, and coatings made by sputtering. Recently, more emphasis has been given to mathematical and numerical modelling of water droplets on superhydrophobic surfaces. However, further work in the modelling area is strongly needed: more emphasis should be given to inclusion of contaminants (now mostly clear water is considered), and to mechanisms other than the two relying on superhydrophobicity. At the present stage, advanced modelling has played a minor role in developing the currently available products; first the lifetime of the commercially available coatings should be improved before more complex approaches will be tried. In detail, Lotus-inspired superhydrophobic surfaces have several disadvantages that hamper practical applications: 1) the micro/nano structures of superhydrophobic surfaces are fragile under the effect of external force, which will result in the degradation of the superhydrophobic

properties; 2) water vapour or moisture, i.e., fog or dew, condensed between the micro/nano structures will also lead to the invalidity of superhydrophobic surface; 3) the air sandwiched between the micro/nano structures is easily replaced by low-surface-tension solutions or compressed under high pressure; 4) micro/nano structures are essential in constructing the superhydrophobic surface, which can reduce the transparency of materials. Consequently, synthesizing robust or self-repairing, transparent, oil or pressure-repellent superhydrophobic surfaces are still urgently needed. It is also to be expected that the ongoing advances in mechanistic insight and modelling will lead to further innovations in design and manufacturing of nature-inspired self-cleaning materials: a truly integrated M3 approach. Superhydrophobic-induced droplet jumping surfaces can well address the issues of water vapour or moisture condensing on superhydrophobic surface, which has been applied in heat transfer. However, compared to Lotus-inspired superhydrophobic surfaces, their structures need to be carefully designed, which will greatly increase their fabricating costs and limit applications. Because of the randomly distributed micro/nano structures, water droplets move on Lotus-inspired surface freely. Butterfly or feather-inspired surfaces are endowed with well-organized structures, resulting in different three-phase contact line (TPCL) or contact angle hysteresis (CAH) for droplets moving on their surface. Thus, the motion of water droplets on this kind of superhydrophobic surfaces can be regulated, which can find potential applications in microfluidics. Underwater superoleophobic surfaces have the advantages of repelling oils or fouling, which is a great improvement compared with superhydrophobic surfaces. However, a limitation is that they can only be applied in water, and not in air. Pitcher-plant-inspired self-cleaning surfaces – infusing liquid into porous structures – have been extensively fabricated and reported. Compared with air, the infused liquid is more difficult to compress and if the infused liquid

is facilitated with low-surface-tension, it can also be superoleophobic. Also, the slippery surface can be transparent. However, the liquid infused in the porous structure is easily removed under the effect of external force, e.g., droplet motion, and gravity force. Thus, maintaining lubricating liquid in the porous structures remains a major challenge. Different from the above self-cleaning surfaces, originating from wettability, gecko-foot-inspired self-cleaning surfaces are mainly attributed to the dynamic asymmetry of van der Waals forces between the dirt particles and clean surfaces. This kind of self-cleaning surface provides a new approach for people to facilitate manipulation of tiny particles as well as demonstrates important impacts on the development of smart and antifouling surfaces, micro-/nano-assemblies, under water cell manipulation technologies, and microelectron mechanical systems devices. Gecko-foot-inspired self-cleaning is based on the dry self-cleaning mechanism; no water should be present.

The research on self-cleaning materials is a multidisciplinary and global effort involving scientists with background in chemistry, physics, materials science, engineering and more. There are already some tens of companies offering commercial self-cleaning coatings, and their number grows every year. The major bottleneck to bring self-cleaning surfaces on the market remains the lack of durability. Coatings usually do not retain non-wetting properties, due to mechanical abrasion, UV degradation or organic contamination. This is the reason why typically the more challenging concepts – based on small-scale synthesis and/or advanced modelling – have not yet been put in practice. This is also the reason that the companies exploiting self-cleaning surfaces are essentially limited to the manufacturers of these coatings. To convince end-user companies to incorporate self-cleaning coatings into their products (e.g. shoes, cars, construction materials) remains a challenge, and likely requires a scientific breakthrough in mechanical durability.

Acknowledgements

This work was supported by European Research Council grant ERC-2016-CoG (725513-SuperRepel) and the Academy of Finland Centres of Excellence Programme 2014-2019.

References

- Aromaa, M., Arffman, A., Suhonen, H., Haapanen, J., Keskinen, J., Honkanen, M., Nikkanen, J.P., Levänen, E., Messing, M.E., Deppert, K., Teisala, H., Tuominen, M., Kuusipalo, J., Stepien, M., Saarinen, J.J., Toivakka, M., Mäkelä J.M., 2012. Atmospheric synthesis of superhydrophobic TiO₂ nanoparticle deposits in a single step using liquid flame spray. *J. Aerosol Sci.* 52, 57-68.
- Attarzadeh, R., Dolatabadi, A., 2017. Coalescence-induced jumping of microdroplets on heterogeneous superhydrophobic surfaces. *Phys. Fluids* 29, 0121014.
- Autumn, K., Liang, Y. A., Hsieh, S. T., Zesch, W., Chan, W.-P., Kenny, W. T., Fearing, R., Full, R. J., 2000. Adhesive force of a single gecko foot-hair. *Nature* 405, 681–685.
- Autumn, K., Sitti, M., Liang, Y.C.A., Peattie, A. M., Hansen, W. R., Sponberg, S., Kenny, T. W., Fearing, R., Israelachvili, J. N., Full, R. J., 2002. Evidence for van der Waals adhesion in gecko setae. *Proc. Natl. Acad. Sci. U. S. A.* 99, 12252–12256.
- Azzopardi, M.J., Brasy, S., 2005. Substrate with a self-cleaning coating. US20050221098A1.
- Ball, P., 1999. Shark skin and other solutions. *Nature* 400, 507–509.
- Barthlott, W., Capesius, I., 1976. Scanning electron-microscopic and functional studies of velamen radicum of orchids. *Ber. Deutsch. Bot. Ges.* 88, 379-390.
- Barthlott, W., Ehler, N., 1977. Raster-Elektronenmikroskopie der Epidermis-Oberflächen von Spermatophyten. *Akad. d. Wiss. ud Literatur.*
- Barthlott, W., Neinhuis, C., 1997. Purity of the sacred lotus, or escape from contamination in biological surfaces. *Planta* 202, 1-8.
- Baum, C., Meyer, W., Stelzer, R., Fleischer, L. G., Siebers, D., 2002. Average nanorough skin surface of the pilot whale (*Globicephala melas*, Delphinidae): considerations on the self-cleaning abilities based on nanoroughness. *Mar. Biol.* 140, 653–657.
- Baughman, R.H., Zakhidov, A.A., Heer, W.A., 2002. Carbon nanotubes-the route toward applications. *Science* 297, 787-792.
- Bhushan, B., Jung, Y.C., 2011. Natural and biomimetic artificial surfaces for superhydrophobicity, self-cleaning, low adhesion, and drag reduction. *Prog. Mater. Sci.* 56, 1-108.
- Blossey, R., 2011. Self-cleaning surfaces-virtual realities. *Nature Mater.* 2, 301-306.
- Bohn, H.F., Federle, W., 2004. Insect aquaplaning: *Nepenthes* pitcher plants capture prey with the peristome, a fully wettable water-lubricated anisotropic surface. *Proc. Natl. Acad. Sci. U. S. A.* 101, 14138-14143.
- Boreyko, J.B., Chen, C.H., 2009. Self-propelled dropwise condensate on superhydrophobic surfaces. *Phys. Rev. Lett.* 103, 184501.
- Born, A.W.; Ermuth, J. 2005. Forming or coating material and utilization thereof. US6919398.
- Bräuer, G., Szyszka, B., Vergöhl, M., Bandorf, R., 2010. Magnetron sputtering-Milestones of 30 years. *Vacuum* 84, 1354-1359.
- Cai, Y., Lin, L., Xue, Z., Liu, M., Wang, S., Jiang, L., 2014. Filefish-inspired surface design for anisotropic underwater oleophobicity. *Adv. Funct. Mater.* 24, 809-816.
- Cao, M., Guo, D., Yu, C., Li, K., Liu, M., Jiang, L., 2015. Water-repellent properties of superhydrophobic and lubricant-infused “slippery” surfaces: a brief study on the functions and applications. *ACS Appl. Mater. Interfaces* 8, 3615-3623.

- Cassell, A.M., Raymakers, J.A., Kong, J., Dai, H., 1999. Large Scale CVD Synthesis of Single-Walled Carbon Nanotubes. *J. Phys. Chem. B* 103, 6484-6492.
- Cassie, A.B.D., Baxter, S., 1944. Wettability of porous surfaces. *Trans. Faraday Soc.* 40, 546–551.
- Chen, H., Zhang, P., Zhang, L., Liu, H., Jiang, Y., Zhang, D., Han, Z.W., Jiang, L., 2016. Continuous directional water transport on the peristome surface of *Nepenthes alata*. *Nature* 532, 85-89.
- Cheng, Y. J., 2005. Is the lotus leaf superhydrophobic? *Appl. Phys. Lett.* 86, 144101.
- Cheng, Q.F., Li, M.Z., Zheng, Y.M., Su, B., Wang, S.T., Jiang, L., 2011. Janus interface materials: superhydrophobic air/solid interface and superoleophobic water/solid interface inspired by a lotus leaf. *Soft Matter* 2011, 7, 5948-5951.
- Chemin, J.B., Bulou, S., Baba, K., Fontaine, C., Sindzingre, T., Boscher, N.D., Choquet, P., 2018. Transparent anti-fogging and self-cleaning TiO₂/SiO₂ thin films on polymer substrates using atmospheric plasma. *Sci. Rep.* 8, 9603.
- Deng, X., Mammen, L., Butt, H.J., Vollmer, D., 2012. Candle Soot as a Template for a Transparent Robust Superamphiphobic Coating. *Science* 335, 67-70.
- Ehiasarian, A.H., Munz, W., 2003. Combined coating process comprising magnetic field-assisted, high power, pulsed cathode sputtering and an unbalanced magnetron. vol. US7981186.
- Farokhirad, S., Morris, J.F., Lee, T., 2015. Coalescence-induced jumping of droplet: Inertia and viscosity effects. *Phys. Fluids* 27, 1021012.
- Feng, L., Li, S.H., Li, Y.S., Li, H.J., Zhang, L.J., Zhai, J., Song, Y.L., Liu, B.Q., Jiang, L., Zhu, D.B., 2002. Super-hydrophobic surfaces: from natural to artificial. *Adv. Mater.* 14, 1857–1860.
- Friedlander S. K., 2000. *Smoke, Dust, and Haze: Fundamentals of Aerosol Dynamics.* (Oxford University Press).
- Gaertner, H.B., 2012. Rotable sputter target. WO2013083205.
- Ganesh, V.A., Raut, H.K., Nair, A.S., Ramakrishna, S., 2011. A review on self-cleaning coatings. *J. Mater. Chem.* 21, 16304-16322.
- Gao, X.F., Yan, X., Yao, X., Xu, L., Zhang, K., Zhang, J.M., Yang, B., Jiang, L., 2007. The dry-style antifogging properties of mosquito compound eyes and artificial analogues prepared by soft lithography. *Adv. Mater.* 19, 2213-2217.
- Gueneau, L., Rondet, M., Besson, S., Boilot, J. P., Gacoin, T., Durand, C., 2009. Substrate with a self-cleaning coating. vol. US7510763.
- Geim, A.K., Dubonos, S.V., Grigorieva, I.V., Novoselov, K.S., Zhukov, A.A., Shapoval, S.Y., 2003. Microfabricated adhesive mimicking gecko foot-hair. *Nature Mater.* 2, 461-463.
- Greene, J.E., 2017. Review Article: Tracing the recorded history of thin-film sputter deposition: From the 1800s to 2017. *J. Vac. Sci. Technol.* 35, 05c204.
- Grill, A.N., Singh, D., 2012. Control of carbon nanotube diameter using CVD or PECVD growth. US8101150.
- Grove, W.R., 1852. VII. On the electrochemical polarity of gases. *Philosophical Transactions of the Royal Society of London.* 142, 87-101.
- Guo, T., Heng, L., Wang, M., Wang, J., Jiang, L., 2016. Robust Underwater Oil-Repellent Material Inspired by Columnar Nacre. *Adv. Mater.* 28, 8505-8510.
- Haapanen, J., Aromaa, M., Teisala, H., Tuominen, M., Stepien, M., Saarinen, J.J., Heikkilä M., Toivakka, M., Kuusipalo, J., Mäkelä J.M. , 2015. Binary TiO₂/SiO₂ nanoparticle coating for controlling the wetting properties of paperboard. *Mater. Chem. Phys.* 149, 230-237.
- Hansen, W.R., Autumn, K., 2005. Evidence for self-cleaning in gecko setae. *Proc. Natl. Acad. Sci. U. S. A.* 102, 385-389.
- Helbig, R., Nickerl, J., Neinhuis, C., Werner, C., 2011. Smart skin patterns protect springtails. *Plos One* 6, e25105.
- Hu. S., Lopez. S., Niewiarowski. P.H., Xia. Z., 2012. Dynamic self-cleaning in gecko

- setae via digital hyperextension. *J. R. Soc. Interface* 9, 2781–2790.
- Israelachvili, J.N., 2015. *Intermolecular and surface forces*. Academic press.
- Jesus, M., Neto, J., Timò G., Paiva, P., Dantas, M., Ferreira, A., 2015. Superhydrophilic self-cleaning surfaces based on TO₂ and TiO₂/SiO₂ composite films for photovoltaic module cover glass. *Appl. Adhes. Sci.* 3, 1-9.
- Kennedy, R.J., 1970. Directional water-shedding properties of feathers. *Nature* 227, 736-737.
- Kim, M.K., Cha, H., Birbarah, P., Chavan, S., Zhong, C., Xu, Y., Miljkovic, N., 2015. Enhanced jumping-droplet departure. *Langmuir* 31, 13452-13466.
- Kong, J., Cassell, A.M., Dai, H., 1998. Chemical vapor deposition of methane for single-walled carbon nanotubes. *Chem. Phys. Lett.* 292, 567-574.
- Kong, J., Soh, H.T., Cassell, A.M., Quate, C.F., Dai, H., 1998. Synthesis of individual single-walled carbon nanotubes on patterned silicon wafer. *Nature* 395, 878-881.
- Kylián, O., Kratochvíl J., Petr, M., Kuzminova, A., Slavíská D., Biederman, H., Beranová J., 2017. Ag/C:F Antibacterial and hydrophobic nanocomposite coatings. *Funct. Mater. Lett.* 10. 1750029.
- Lafuma, A., Quéré D, 2011. Slippery pre-suffused surfaces. *EPL (Europhysics Letters)*, 96, 56001.
- Lau, K.K., Bico, J., Teo, K.B., Chhowalla, M., Amaratunga, G. A., Milne, W. I., Mckinley, G.H., Gleason, K.K., 2003. Superhydrophobic carbon nanotube forests. *Nano Lett.* 3, 1701-1705.
- Lee, J., Fearing, R.S., 2008. Contact self-cleaning of synthetic gecko adhesive from polymer microfibers. *Langmuir* 24, 10587-10591.
- Lee, Y.H., Lee, N.S., Kim, J.M., 2004. Method of vertically aligning carbon nanotubes on substrates at low pressure using thermal chemical vapor deposition with DC bias. US6673392.
- Liu, F., Ghigliotti, G., Feng, J.J., Chen C-H., 2014. Numerical simulations of self-propelled jumping upon drop coalescence on non-wetting surfaces. *J. Fluid Mech.* 752, 39-65.
- Liu, K., Du, J., Wu, J., Jiang, L., 2012. Superhydrophobic gecko feet with high adhesive forces towards water and their bio-inspired materials. *Nanoscale* 4, 768-772.
- Liu, M., Wang, S., Wei, Z., Song, Y., Jiang, L., 2009. Bioinspired design of a superoleophobic and low adhesive water/solid interface. *Adv. Mater.* 21, 665-669.
- Liu, Y., Choi, C.H., 2013. Condensation-induced wetting state and contact angle hysteresis on superhydrophobic lotus leaves. *Colloid Polym. Sci.* 291, 437-445.
- Madocks, J.M., Ngo, P., 2010. Rotary magnetron magnet bar and apparatus containing the same for high target utilization. US9388490.
- Marmur, A., 2012. Hydro-hygro-oleo-omni-phobic? Terminology of wettability classification. *Soft Matter* 8, 6867-6870.
- Masson, G., Kaizuka, I., Lindahl, J., Jaeger-Waldau, A., Neubourg, G., Ahm, P., Donose, J. Tilli, F., 2018. A snapshot of global PV markets-the latest survey results on PV markets and policies from the IEA PVPS Programme in 2017. *IEEE*.
- Masuda, Y., Kato, K., 2013. Superhydrophilic SnO₂ nanosheet-assembled film. *Thin Solid Films* 544, 567-570.
- Müller, L., 2004. Liquid-fed Aerosol Reactors for One-step Synthesis of nanostructured Particles. *KONA* 22, 14.
- Müller, L.; Kammler, H.K.; Mueller, R.; Pratsinis, S.E.; 2002. Controlled synthesis of nanostructured particles by flame spray pyrolysis. *J. Aerosol. Sci.* 33, 369-389.
- Müller, L.; Stark, W.J.; Pratsinis, S.E.; 2002. Flame-made Ceria Nanoparticles. *J. Mater. Res.* 17, 1356-1362.
- Müller, L., Roessler, A., Pratsinis, S.E., Sahm, T., Gurlo, A., Barsan, N., Weimar, U., 2006. Direct formation of highly porous gas-sensing films by in situ

- thermophoretic deposition of flame-made Pt/SnO₂ nanoparticles. *Sens. Actuat. B-Chem.* 114, 283-295.
- Mei, H., Luo, D., Guo, P., Song, C., Liu, C., Zheng, Y., Jiang, L., 2011. Multi-level micro-/nanostructures of butterfly wings adapt at low temperature to water repellency. *Soft Matter* 7, 10569–10573.
- Mengüç, Y., Rohrig, M., Abusomwan, U., Holscher, H., Sitti, M., 2014. Staying sticky: contact self-cleaning of gecko-inspired adhesives. *J. R. Soc. Interface* 11, 20131205.
- Miljkovic, N., Enright, R., Nam, Y., Lopez, K., Dou, N., Sack, J., Wang, E., 2013. Jumping-droplet-enhanced condensation on scalable superhydrophobic nanostructured surfaces. *Nano Lett.* 13, 179-187.
- Müller, R.; Mäller, L.; Pratsinis, S.E., 2003. Nanoparticle synthesis at high production rates by flame spray pyrolysis. *Chem. Eng. Sci.* 58, 1969-1976.
- Müller -Steinhagen, H., Malayeri, M., Watkinson, A., 2005. Fouling of heat exchangers-new approaches to solve an old problem. *Heat Transfer Eng.* 26, 1-4.
- Müller -Steinhagen, H., Malayeri, M., Watkinson, A., 2009. Heat exchanger fouling: Environmental impacts. *Heat Transfer Eng.* 30, 773-776.
- Neinhuis, C., Barthlott, W., 1997. Characterization and distribution of water-repellent, self-cleaning plant surfaces. *Ann. Bot.* 79, 667–77.
- Nghiem, B., Zagdoun, G., Sondergard, E., Garrec, R., Royer, E., Kharchenko, A., Lelarge, A., Barthel, E., 2011. Antifouling material and production method thereof. US7955687B2.
- Nun, E.O., Schleich, B., 2007. Surface rendered self-cleaning by hydrophobic structures and a process for their production. US7211313.
- Nun, E. O., 2006. Verwendung von mit fluorsilanen hydrophobierten Partikeln zur Herstellung von selbstreinigenden Oberflächen mit lipophoben, oleophoben, laktophoben und hydrophoben Eigenschaften. EP163066.
- Pakdel, E., Daoud, W.A., Wang, X.G., 2013. Self-cleaning and superhydrophilic wool by TO₂/SiO₂ nanocomposite. *Appl. Surf. Sci.* 275, 397-402.
- Parkin, I.P., Palgrave, R.G., 2005. Self-cleaning coatings. *J. Mater. Chem.* 15, 1689-1695.
- Price, J., 2012. In-vacuum rotational device. WO2013104925.
- Quéé D., 2008. Wetting and roughness. *Annu. Rev. Mater. Res.* 38, 71-99.
- Renevier, N.M., Fox, V.C., Teer, D.G., Hampshire, J., 2000. Coating characteristics and tribological properties of sputter-deposited MoS₂/metal composite coatings deposited by closed field unbalanced magnetron sputter ion plating. *Surf. Coat Tech.* 127, 24-37.
- Russell, A.P., 1975. A contribution to the functional morphology of the foot of the tokay, Gekko gekko (Reptilia, Gekkonidae). *J. Zool. Lond.* 176, 437-476.
- Salameh, S., Schneider, L., Laube, J., Alessandrini, A., Facci, P., Seo, J.W., Colmbi, C.L., Mäller, L., 2012. Adhesion mechanisms of the contact interface of TiO₂ Nanoparticles in Films and Aggregates. *Langmuir* 28, 11457-11464.
- Sahm, T., Mäller, L., Gurlo, A., Barsan, N., Pratsinis, S.E., Weimar, U., 2004. Flame spray synthesis of tin dioxide nanoparticles for gas sensing. *Sens. Actuat. B-Chem.* 98, 148-153.
- Sahm, T., Rong, W., Bälller, L., Friedlander, S.K., Weimar, U., 2007. Formation of multilayer films for gas sensing in situ thermophoretic deposition of nanoparticles from aerosol phase. *J. Mater. Res.* 22, 850-857.
- Sarkar, S., Pradhan, S. K., 2014. Tailoring of optical and wetting properties of sputter deposited silica thin films by glancing angle deposition. *Appl. Surf. Sci.* 290, 509-513.
- Schaffer, M.W., Johnson, B., Geng, J., Shephard, D., Singh, C., 2004. CVD synthesis of carbon nanotubes. US8173211.
- Schill, R., Barthlott, W., Ehler, N., 1973. Cactus spines under the electron scanning

- microscope. *Cactus Succulent J.* XLV, 175-185.
- Schopf, S.O., Salameh, S., Muller, L., 2013. Transfer of highly porous nanoparticle layers to various substrates through mechanical compression. *Nanoscale* 5, 3764-3772.
- Simpson, J.T., Ivanov, I., Shibata, J., 2012. Self-cleaning skin-like prosthetic polymer surfaces. US8142516.
- Smith, J.D., Dhiman, R., Anand, S., Reza-Garduno, E., Cohen, R.E., McKinley, G. H., Varanasi, K.K., 2013. Droplet mobility on lubricant-impregnated surfaces. *Soft Matter* 9, 1772-1780.
- Soeren, P.M., Poulsen H., Gunnarson, S.G., 2009. WO2010069997A1.
- Stark, W. J., Pratsinis, S. E., 2002. Aerosol flame reactors for manufacture of nanoparticles. *Powder Technol.* 126, 103-108.
- Stepien, M., Saarinen, J.J., Teisala, H., Tuominen, M., Aromaa, M., Haapanen, J., Kuusipalo, J., Makela, J.M., Toivakka, M., 2013. Tof-SIMS analysis of UV-switchable TiO₂ nanoparticle-coated paper surface. *Langmuir* 29, 3780-3790.
- Stepien, M., Saarinen, J.J., Teisala, H., Tuominen, M., Aromaa, M., Haapanen, J., Kuusipalo, J., Makela, J.M., Toivakka, M., 2013. Compressibility of porous TiO₂ nanoparticle coating on paperboard. *Nanoscale Res. Lett.* 8, 444.
- Stepien, M., Saarinen, J.J., Teisala, H., Tuominen, M., Kuusipalo, J., Makela, J.M., Toivakka, M., 2012. Surface chemical analysis of photocatalytic wettability conversion of TiO₂ nanoparticle coating. *Surf. Coat Technol.* 208, 73-79.
- Su, M., Zheng, B., Liu, J., 2000. A scalable CVD method for the synthesis of single-walled carbon nanotubes with high catalyst productivity. *Chem. Phys. Lett.* 322, 321-326.
- Teoh, W.Y., Amal, R., Muller, L., Pratsinis, S.E., 2007. Flame sprayed visible light-active Fe-TiO₂ for photomineralisation of oxalic acid. *Catal. Today* 120, 203-213.
- Tricoli, A., Righettoni, M., Pratsinis, S.E., 2009. Anti-fogging nanofibrous SiO₂ and Nanostructured SO₂-TiO₂ films made by rapid flame deposition and in situ annealing. *Langmuir* 25, 12578-12584.
- Tulli, D., Mazumder, P., Infante, D., Carrilero, A., Pruneri, V., 2013. Superhydrophobic Sputtered Al₂O₃ Coating Films with High Transparency. In *The European Conference on Lasers and Electro-Optics* (p. CE_2_1). Optical Society of America.
- Vahabi, H., Wang, W., Davies, S., Mabry, J.M., Kota, A.K., 2017. Coalescence-induced self-propulsion of droplets on superomniphobic surfaces. *Appl. Mater. Interfaces* 9, 29328-29336.
- Vahabi, H., Wang, W., Mabry, J.M., Kota, A.K., 2018. Coalescence-induced jumping of droplets on superomniphobic surfaces with macrotecture. *Science Advances*, 4, eaau3488.
- Volder, M.F.L., Tawfick, S.H., Baughman, R.H., Hart, A.J., 2013. Carbon nanotubes: present and future commercial applications. *Science* 339, 535.
- Vollmer, D., Butt, J., Klapper, M., D'Acunzi, M., Mammen, Lena., Xu, D., 2012. Mechanical stable, transparent, superhydrophobic, and oleophobic surfaces made of hybrid raspberry-like particles. EP 2484726A1.
- Wang, K., Liang, Q., Jiang, R., Zheng, Y., Lan, Z. and Ma, X., 2017. Numerical simulation of coalescence-induced jumping of multidroplets on superhydrophobic surfaces: initial droplet arrangement effect. *Langmuir* 33, 6258-6268.
- Wang, K., Liang, Q., Jiang, R., Zheng, Y., Lan, Z. and Ma, X., 2017. Critical size ratio for coalescence-induced jumping on superhydrophobic surfaces. *Appl. Phys. Lett.* 111, 061603.
- Wang, Q., Yao, X., Liu, H., Que D., & Jiang, L. 2015. Self-removal of condensed water on the legs of water striders. *Proc. Natl. Acad. Sci. U. S. A.* 112, 9247-9252.
- Watson, G.S., Cribb, B.W., Watson, J.A., 2010. How micro/nanoarchitecture

- facilitates anti-wetting: an elegant hierarchical design on the termite wing. *ACS Nano* 4, 129-136.
- Watson, J.A., Cribb, B.W., Hu, H.M., Watson, G.S., 2011. A dual layer hairy array of the brown lacewing: Repelling water at different length scales. *Biophys. J.* 100, 1149-1155.
- Wegner, K., Pratsinis, S.E., 2003. Scale-up of nanoparticle synthesis in diffusion flame reactors. *Chem. Eng. Sci.* 58, 4581-4589.
- Wenzel, R.N., 1936. Resistance of solid surfaces to wetting by water. *Ind. Eng. Chem.* 28, 988-994.
- Wisdom, K.M., Watson, J.A., Qu, X., Liu, F., Watson, G.S., Chen, C.H., 2013. Self-cleaning of superhydrophobic surfaces by self-propelled jumping condensate. *Proc. Natl. Acad. Sci. U. S. A.* 110, 7992-7997.
- William, L.T., John, S.A., Jeffrey, A.F., Kevin, B.K., Gary, J. D., George, A.N., Brett, R.F., 2006. Electrochromic device having a self-cleaning hydrophilic coating with a controlled surface morphology. WO2006121659A1.
- Wong, T. S., Kang, S.H., Tang, S.K., Smythe, E.J., Hatton, B.D., Grinthal, A., Aizenberg, J., 2011. Bioinspired self-repairing slippery surfaces with pressure-stable omniphobicity. *Nature* 477, 443-447.
- Xiao, L.L, Li, J.S., Mieszkin, S., Di Fino, A., Clare, A. S., Callow, M. E., Callow, J.A., Crunze, M., Rosenhahn, A., Levkin, P. A., 2013. Slippery liquid-infused porous surfaces showing marine antibiofouling properties. *ACS Appl. Mater. Interfaces* 5, 10074-10080.
- Xiu, Y., Zhu, L., Hess, D.W., Wong, C.P., 2006. Biomimetic creation of hierarchical surface structures by combining colloidal self-assembly and Au sputter deposition. *Langmuir* 22, 9676-9681.
- Xu, Q., Wan, Y., Hu, T., Tao, D., Niewiarowski, P., Tian, Y., Liu, Y., Dai, Li., Yang, Y., Xia, Z., 2015. Robust self-cleaning and micromanipulation capabilities of gecko spatulae and their bio-mimics. *Nat. Commun.* 6, 8949.
- Xue, Z., Wang, S., Lin, L., Chen, L., Liu, M., Feng, L., Jiang, L., 2011. A novel superhydrophilic and underwater superoleophobic hydrogel-coated mesh for oil/water separation. *Adv. Mater.* 23, 4270-4273.
- Yahyazadeh, A., Khoshandam, B., 2017. Carbon nanotube synthesis via the catalytic chemical vapor deposition of methane in the presence of iron, molybdenum, and iron-molybdenum alloy thin layer catalysts. *Results Phys.* 7, 3826-3837.
- Yan, Y., Miao, J., Yang, Z., Xiao, F. X., Yang, H. B., Liu, B., Yang, Y., 2015. Carbon nanotube catalysts: recent advances in synthesis, characterization and applications. *Chem. Soc. Rev.* 44, 3295-3346.
- Yao, L., He, J., 2014. Recent progress in antireflection and self-cleaning technology-From surface engineering to functional surfaces. *Prog. Mater. Sci.* 61, 94-143.
- Zhao, X., Zhao, Q., Yu, J., Liu, B., 2008. Development of multifunctional photoactive self-cleaning glasses. *J. Non-Cryst. Solids* 354, 1424-1430.
- Zhao, H., Sun, Q., Deng, X., Cui, J., 2018. Earthword-inspired rough polymer coatings with self-replenishing lubrication for adaptive friction-reduction and antifouling surfaces. *Adv. Mater.* 30, 1802141.
- Zeman, P., Takabayashi, S., 2002. Self-cleaning and antifogging effects of TiO₂ films prepared by radio frequency magnetron sputtering. *J. Vac. Sci. Technol. A* 20, 388-393.
- Zhang, F., Jiang, L., Wang, S., 2018. Repairable cascaded slide-lock system endows bird feathers with tear-resistance and superdurability. *Proc. Natl. Acad. Sci. U. S. A.* 115, 10046-10051.
- Zhang, R., Amlani, I., Baker, J., 2004. Chemical vapor deposition of single walled carbon nanotubes. WO2004070854A1.
- Zheng, L., Zhang, X., Li, Q., Chikkannavar, S., Li, Y., Zhao, Y.,

- Liao, X., Jia, Q., Doorn, S., Peterson, D., Zhu, Y., 2007. Carbon-nanotube cotton for large-scale fibers. *Adv. Mater.* 19, 2567-2570.
- Zheng, Y., Gao, X., Jiang, L., 2007. Directional adhesion of superhydrophobic butterfly wings. *Soft Matter* 2007, 3, 178-182.
- Zhu, W., Pratsinis, S.E., 1997. Synthesis of SiO_2 and SnO_2 particles in diffusion flame reactors. *AIChE J.* 43, 2657-2664.